Energy 187 (2019) 115917

Contents lists available at ScienceDirect

Energy

journal homepage: www.elsevier.com/locate/energy

Enhancement of maximum power output through reconfiguration techniques under non-uniform irradiance conditions

G.Sai Krishna*, Tukaram Moger

Department of Electrical & Electronics Engineering NIT Karnataka, Surathkal India

ARTICLE INFO

Article history:
Received 20 April 2019
Received in revised form
5 August 2019
Accepted 8 August 2019
Available online 13 August 2019

Keywords:
PV modelling
Partial shading conditions (PSCs)
And reconfiguration strategies

ABSTRACT

Partial shading is one of the major drawback which diminishes the power output of the PV array. One of the effective methodologies is reconfiguration strategies, namely shifting the location of PV modules from one place to different places so as to distribute shading effects over the array to increase maximum power output under PSCs. This paper proposed two novel puzzle arrangements followed by Ken-Ken (KK) and Skyscraper (SS) for 4×4 total-cross-tied (TCT) PV array and increase maximum power under PSCs. In this approach, the PV modules in the TCT array is arranged according to Ken-Ken and Skyscraper arrangements without changing the electrical connections. Further, the performance of the proposed arrangements are investigated with different existing PV array configurations by comparing the global maximum power point (GMPP), the voltage at global maximum power point (V_{GMPP}), mismatch losses (ML), fill-factor (FF), efficiency (η) and possible local peaks (PLP) under different shading patterns using Matlab-Simulink. An extensive simulation study is carried out on these configurations under different shading patterns as well as temperatures. Also, a comprehensive comparison has done for various reconfiguration schemes presented in literature. The result shows that the proposed arrangements are enhancing the global maximum power as compared to the other existing configurations.

1. Introduction

Photovoltaic (PV) system is widely used as a source of green energy due to its ability to directly convert solar energy into electrical energy [1,2]. Shading phenomena which can be directly affect the PV modules' output current and maximum power, thus lowering the effectiveness of the whole PV system. Shading can occur due to the shades of passing clouds, tress, flying birds, near buildings, some portion of PV modules may get less intensity of solar irradiance as compared to unshaded portion, which causes reduction in output power [3]. Under this condition, the shaded modules are consuming the power instead of generating, thus creates hot-spot in PV array; further, it may damage the PV modules. One of the approaches is PV array interconnections to reduce PSCs. Various array interconnections put forth in the literature to obtain improved performance such as "series-parallel(SP), total-cross-tied(TCT), bridge-link(BL) and honey-comb(HC)" [4–7]. As per the literature, TCT array offers highest maximum power and shows less susceptibility to PSCs as compared to the other interconnections [6,8,9]. The major issue with the TCT configuration is if the number of PV modules are shaded in a row, that limits the output current of the PV array [10]. However, to solve this issue, many authors have been proposed reconfiguration strategies for TCT PV array in order to distribute shading effects from one place to different places uniformly, thereby minimizing the mismatch losses [11,12]. Based on the literature, these strategies can be classified into dynamic and static reconfiguration techniques.

In dynamic technique, PV modules are reconfigured dynamically within the PV array to increase maximum power output under PSCs. In Refs. [15,16], an Electrical Array Reconfiguration (EAR) controller is developed to change the connections between among the PV modules based on irradiance levels for providing input current to the motor. In Ref. [17], a new adaptive PV cell array technique is proposed to reduce PSCs. It consists of a fixed part, adaptive part, and the switching matrix. In this technique, the switching matrix plays a crucial role to connect adaptive PV cells into the fixed cells to compensate irradiance drop in each row [18]. Still, various papers [11,19,20] have been reported based on dynamic reconfiguration approach to reduce PSCs. According to literature, the dynamic reconfiguration technique requires sensors

* Corresponding author.
E-mail address: saikrishna240@gmail.com (G.Sai Krishna).

https://doi.org/10.1016/j.energy.2019.115917
0360-5442/

Notations

$V_{cell/m/a}$	: PV cell/module/array voltage (V)
$I_{cell/m/a}$	: PV cell/module/array current(A)
I_d	: diode current of a PV cell
I_{sh}	: shunt current of the PV cell
T_c	: PV module operating temperature
T_{STC}	: standard operating temperature at 298.15K
I_o	: saturation current of the cell
K_{isc}	: short-circuit current temperature co-efficient
n	:ideality factor
k	: boltzmann's constant 1.3805×10^{-23}J/K
q	: electron charge 1.6×10^{-19}C
G	:actual Irradiance of PV module

to identify the shading and faulty conditions, reconfiguration algorithm to optimize the best possible connection to get higher maximum power and switching matrix to connect the switching between PV modules. The set of components would increase the cost of the technique, as well as the configuration of the system [11,19,20].

Static technique utilizes a fixed interconnection scheme, it means the physical location of PV modules is shifting in PV array without altering the electrical connections. However, this technique doesn't require any sensors, reconfiguration algorithm, and the switching matrix as in case of dynamic technique. The most challenging part of this technique is to choose an effective reconfigurable pattern to distribute shading effects over the array. In Ref. [21], proposed 9×9 SuDoKu pattern arrangement for TCT to improve maximum power output under PSCs. In this approach, the physical location of PV modules in TCT array is arranged in a SuDoKu manner. Consequently, the authors in Ref. [22] developed an optimal SuDoKu arrangement for TCT to increase the global maximum power output. During the study, it is observed that the proposed arrangement is minimizing the mismatch losses as compared to SuDoKu arrangement [21]. In Ref. [13], they proposed a Magic-Square (MS) arrangement to distribute partial shading effects on 4×4 PV array. In this approach, the physical location of PV modules is arranged in a magic-square manner. This paper indicates that the proposed arrangement is increasing the global maximum power as compared to the SP, TCT, BL, HC along with SP-TCT and BL-TCT PV array configurations under most shading cases. In Ref. [14], proposed a symmetrical Latin-Square (LS) arrangement for 4×4 TCT array to distribute various partial shading conditions. In this study, the authors have considered various parameters to verify the proposed arrangement under each shading condition. However, the obtained result shows that the proposed arrangement enhancing the global maximum power as compare to the TCT. However, as per observation from the papers [13,14], few shortcomings are found; (i) The first column of the patterns remains unaltered (see Fig. 1, highlighted). It means, if the shadow falls on the left side of the array it will remain undistributed. Hence, this lead to reduction in power output. (ii) In Ref. [14], the pattern has issue with the repeated row-wise PV modules in the diagonal i.e., 1^{st} row of the PV modules 11,12,13 and 14 are connected in diagonal is shown in Fig. 1. If the shading occurs in diagonal, as a result of that, it increases the shaded PV modules in the same row (i.e. after shading dispersion), further, it reduces the output current of the array. Still, many authors have been reported various reconfigurable patterns in the open-literature to reduce PSCs, which are presented in Table 1.

Novelty of this study.

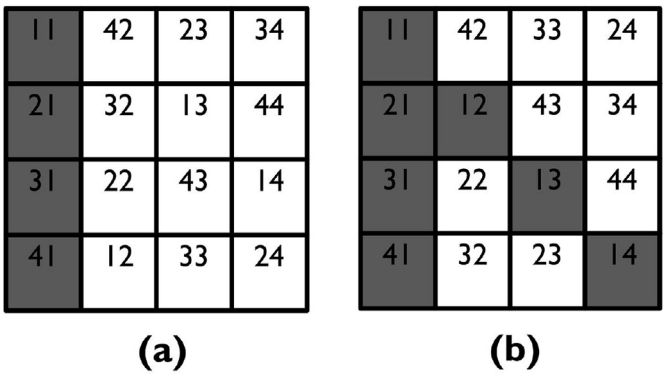

Fig. 1. PV array patterns:(a) Magic-Square (MS) [13], (b) Latin-Square (LS) [14].

- With respect to the literature, this paper proposed two novel puzzle arrangements i.e., Ken-Ken (KK) and Skyscraper (SS) for 4×4 TCT PV array based on only changing the physical location of the modules without altering the connections to enhance maximum power under PSCs. So that the shading effects will distribute uniformly over the array, further, the power output can be improved.
- The performance of the proposed arrangements are investigated with existing configurations such as "SP, TCT, BL, HC, Magic-Square (MS) [13] and Latin-Square (LS) [14]" by comparing the GMPP, V_{GMPP}, mismatch losses (ML), fill factor (FF), efficiency (η) and possible local peaks (PLP) under various shading patterns.

In Fig. 2, shows that PV array configurations, partial shading conditions, and the performance investigation parameters considered in this paper.

The structure of the paper as follows; Section 2, presents mathematical modelling of PV array. In Section 3.2, discussed about formation of Ken-Ken and Skyscraper puzzle and pattern arrangements. In Section 3.4, description of various partial shading conditions. Section 4, result and discussion part for the proposed arrangements and followed by the conclusion is presented in Section 5.

2. Mathematical modelling of PV array

Modelling of the PV array starts with the mathematical modelling of a single solar cell [32]. Various types of solar cells are reported in the open literature, but the single diode PV cell model is quite simple as compared to the other existing models [33]. The equivalent circuit of a single diode PV cell model is shown in Fig. 3.

By applying KCL to node 'c' in Fig. 3, I_{cell} can be written as,

$$I_{cell} = I_{Lcell} - I_d - I_{sh} \tag{1}$$

where I_{Lcell} is light generated current of the PV cell. The general representation of PV cell output characteristics is given by,

$$I_{cell} = I_{Lcell} - I_o\left[exp\left\{\frac{q(V_{cell} + I_{cell}R_s)}{kaT_c} - 1\right\}\right] - \frac{(V_{cell} + I_{cell}R_s)}{R_{sh}} \tag{2}$$

PV module is composed by connecting the number of solar cells in series(n_s). The PV module output current equation is given in Eq. (3),

Table 1
Taxonomy of static PV array reconfiguration techniques with TCT PV array.

authors	proposed pattern	array level	shading conditions	power output	remarks
[23]	Optimal Su-Do-Ku	9 × 9	Horizontal diagonal bottom left bottom right	4320 W	Optimal Su-Do-Ku arrangement showing best results than TCT
[24]	static shade tolerant scheme	3 × 3, 5 × 5	Horizontal, vertical,etc	1200 W	Renumbering the PV modules before the connections to disperse PSCs
[25]	Shadow Dispersion Scheme	7 × 7	SW,LN,center,L, one module patterns	3600 W	Renumbering the PV modules before the connections to disperse PSCs
[26]	shade dispersion positioning Scheme	3 × 3	different shadings	1500 W	Renumbering the PV modules before the connections to disperse PSCs
[27]	Adjacent shifting pattern	9 × 9	SW,LW,SN, LN	2800 W	Adjacent shifting arrangement can deduct the PSCs
[28]	dominance-square pattern	5 × 5	SW,LW,SN, LN	4800 W	Dominance square arrangement enhance the power output of TCT array
[29]	Column Index (CI) arrangement	9 × 9	SW,LW,SN, LN	5200 W	Proposed column index (CI) arrangement for TCT to disperse PSCs
[30]	Cross Diagonal View (CDV)	9 × 9	Inner and diagonal shadings	9200 W	proposed CDV arrangement for TCT to disperse shading effects
[31]	Two phase reconfiguration	9 × 9	SW,LW,SN, LN	7800 W	Two phase reconfiguration for shaded dispersion in TCT array

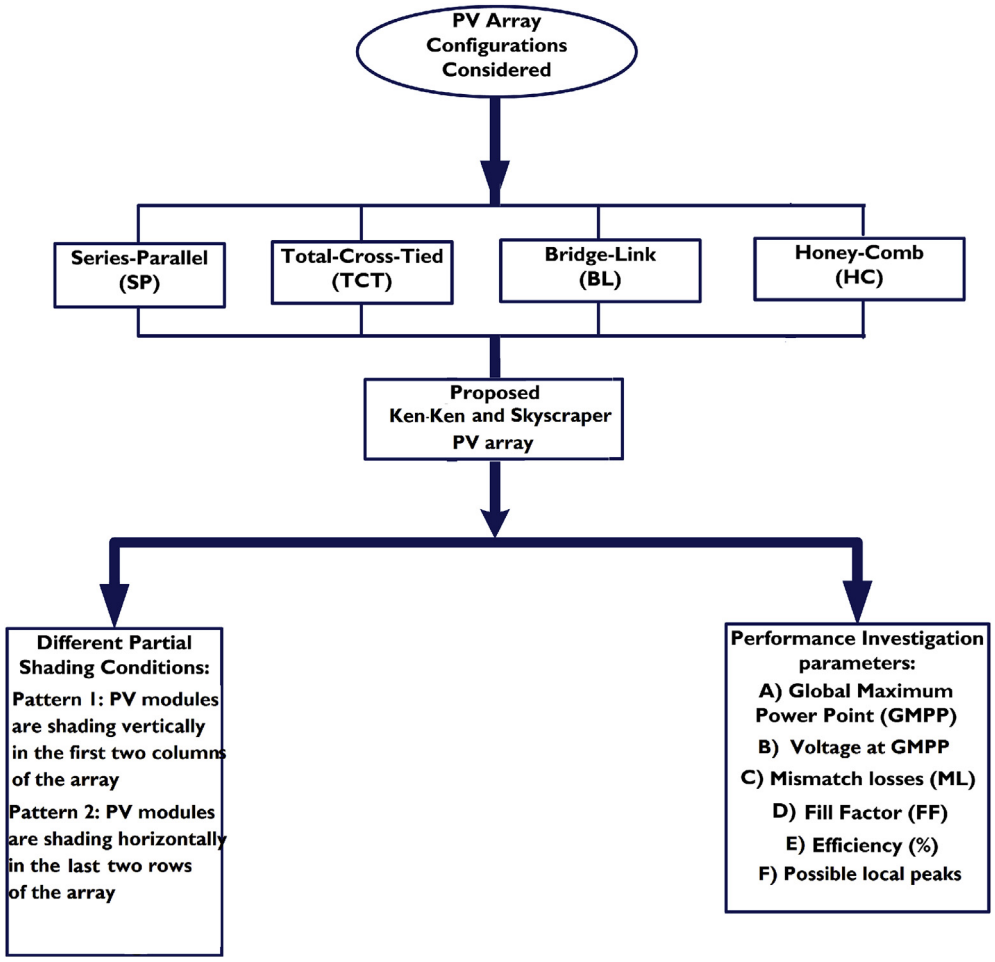

Fig. 2. State of the art: PV configurations, PSCs and performance parameters.

$$I_m = I_L - I_o\left[exp\left\{\frac{q(V_m + I_m R_S)}{n_s k a T_c} - 1\right\}\right] - \frac{(V_m + I_m R_S)}{R_{SH}} \quad (3)$$

where I_L is light generated current of the module, which can be written as,

$$I_L = \frac{G}{G_o}\left[I_{L_{STC}} + K_{isc}(T_c - T_{STC})\right] \quad (4)$$

Eq. (3) is a transcendental equation, this can also be extended to calculate the array current by connecting PV modules in series (N_S) and parallel (N_P) as shown in Fig. 4. The I–V characteristics equation for the PV array is given in Ref. [34], which can be represented as.

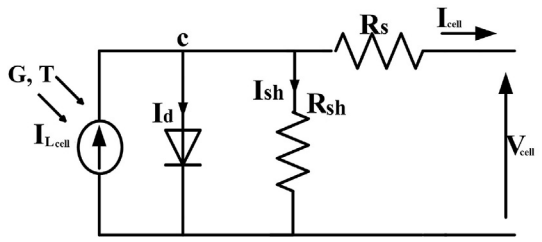

Fig. 3. Single diode PV cell model.

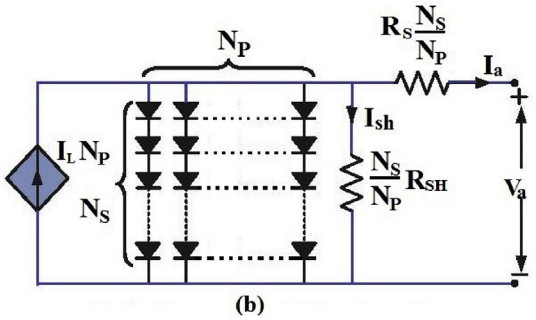

Fig. 4. Formation of PV array.

$$I_a = N_P.I_L - N_P.I_o exp\left\{\frac{q\left(V_a + \frac{N_S}{N_P}I_a R_S\right)}{N_S k a T_c} - 1\right\} - \frac{\left(V_a + \frac{N_S}{N_P}I_a R_S\right)}{\frac{N_S}{N_P}R_{SH}} \quad (5)$$

The above set of equations are used to model the PV array to simulate I–V and P–V characteristics with the help of data sheet parameters is presented in Ref. [7].

2.1. Total-cross-tied PV array configuration

In TCT, first PV modules are connected in parallel to make tiers. In similar way, all tiers are connected in series. The general layout of TCT array is shown in Fig. 5. It consists of 16 PV modules, assembled into four rows and four columns. In each row, four PV modules are connected in parallel, the voltage across each row is equal to open-circuit voltage of the single PV module. The output voltage of an array is equal to the sum of row voltages, it can find by applying Kirchhoff's Voltage Law (KVL) to Fig. 5,

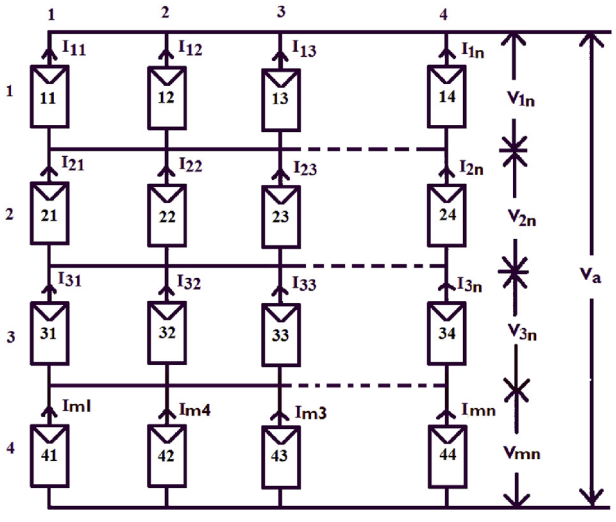

Fig. 5. TCT PV array Configuration.

$$V_a = \sum_{p=1}^{4} V_{mp} \quad (6)$$

where V_{mp} is referred to maximum voltage at the p^{th} row. However, the array current is equal to the sum of modules current which are connected in parallel in a single row; this can be calculated by applying KCL to each node in Fig. 5, the output current I_a can be expressed as [21];

$$I_a = \sum_{q=1}^{4}\left(I_{pq} - I_{(p+1)q}\right) = 0 \quad p = 1, 2, \ldots 4 \quad (7)$$

where p and q are the number of rows and columns of the array. The 4×4 SP, BL and HC PV array configurations are shown in Fig. 6.

3. Proposed puzzle and pattern arrangements

3.1. Ken-Ken (KK) puzzle

Ken-Ken (KK) is a logic-based number placement puzzle and is a family of SuDoKu.This puzzle consists of m × n grid, which contains square blocks (Y) surrounded by bold lines. The objective of this puzzle is to place the numbers 1 to N in the array without repeating the same number in a row or column. The formation of this puzzle is entirely based on simple arithmetic operations such as addition (+), subtraction(−), division (÷) and multiplication (×). In m × n grid, each sub-grid split into different blocks and each of those blocks have arithmetic operations associated as shown in Fig. 7(a). To solve this grid that the numbers in each block equal to the arithmetic operations assigned to it. In Fig. 7(a), it consists of 16 blocks constituted as four rows and four columns. Each sub-grid block is performed arithmetic operations within it to fill the empty blocks. The following steps are performed to fill the empty blocks are as follows.

(i) Step 1: block 1 contains digit 5 with an addition operation, the way to get this digit using the same operation is of 2 + 3 is shown in Fig. 7(b)
(ii) Step 2: block 2 contains digit 7 with an addition operation, the way to get this digit using the same operation is of 3 + 4, since digit 3 is already exist in the row so that to fill with 4 + 3 is shown in Fig. 7(c)
(iii) Step 3: Similarlly, block 3 contains digit 8 with multiplication operation, so that to fill with 2 × 4 is shown in Fig. 7(d)

Similarly, fill all the empty blocks using arithmetic rules. The 4 × 4 Ken-Ken puzzle and pattern arrangement are shown in Fig. 8(a)& (b) respectively.

3.2. Skyscraper (SS) puzzle

Skyscraper(SS) is a logic-based number placement puzzle, is a one of the method of SuDoKu. This puzzle consists of m × n grid with clues along its sides. In the grid, each square box referred to skyscraper. The main objective of this puzzle is to place a skyscraper in each box with the heights between 1 to N. So that, the same height skyscrapers are not able to repeat in a row or column. The 4 × 4 Skyscraper puzzle is shown in Fig. 9(a). The number indicates

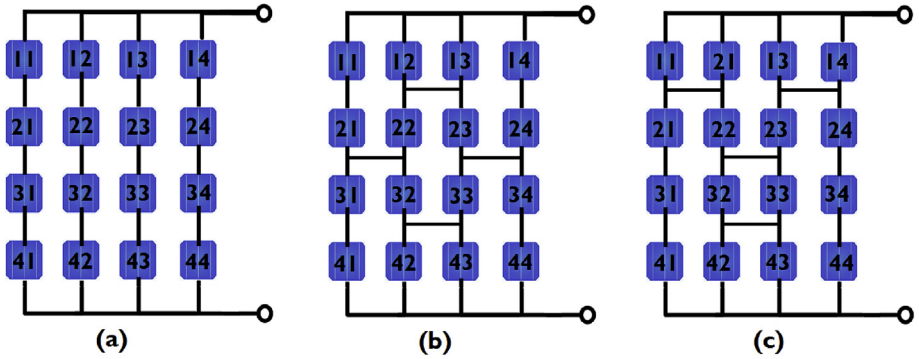

Fig. 6. PV array configurations: (a) SP, (b) BL and (c) HC.

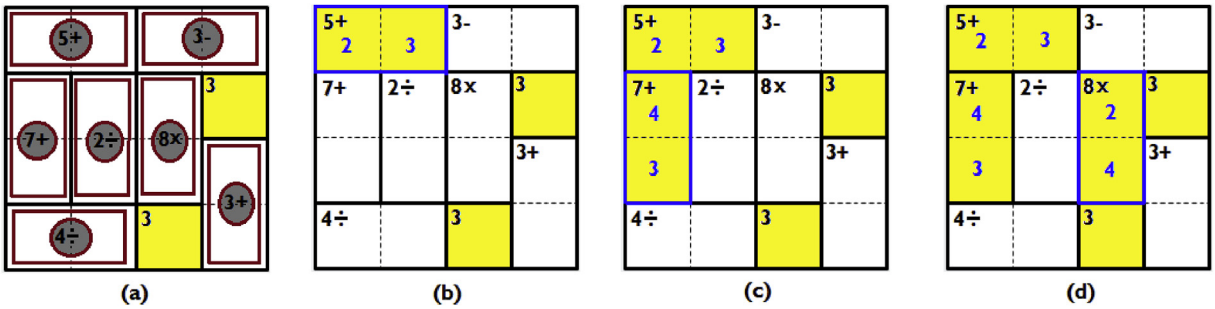

Fig. 7. Formation of Ken-Ken puzzle: (a) 4 × 4 grid with arithmetic operations, (b) fill the block 1 using addition operation (highlighted in yellow), (c) fill the block 2 using addition operation, and (d) fill the block 3 using multiplication operation.

outside that box is the clue, which tells how many skyscrapers are visible from that place. The number of visible skyscrapers viewed from the direction of each clue, is equal to the value of the clue.

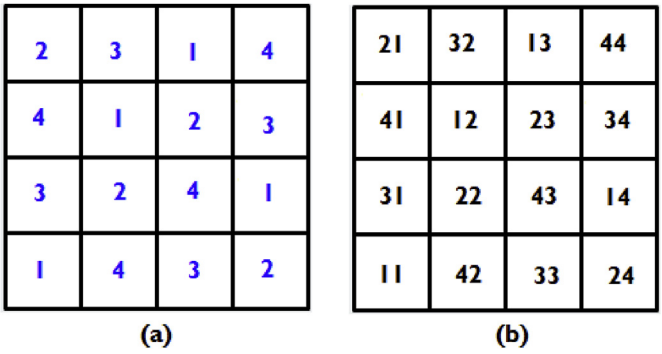

Fig. 8. (a) 4 × 4 Ken-Ken puzzle and (b) Ken-Ken pattern arrangement.

In Fig. 9(a), it consists of 16 square boxes and each box listed with one clue, which tells direction of the view. The following steps give the way to fill the boxes.

(i) Step 1: The 'clue 4′ tells that four skyscrapers are visible at that position and is filled with 1–4 in the order is shown in Fig. 9(b) (Note: Higher skyscraper hide the view of shorter skyscraper located behind them).
(ii) Step 2: 'clue 1′ says that only one skyscraper is visible from that view and which must be the < 4 > is given in Fig. 9(c).
(iii) Step 3: 'clue 2′ tells that two skyscrapers are visible from that point of view and which must be < 3 > and < 4 > ; otherwise if < 1 > it shows four skyscrapers shown in Fig. 9(d).

The remaining boxes are filled based on given clues. The final Skyscraper puzzle and pattern arrangement are shown in Fig. 10(a)&(b) respectively.

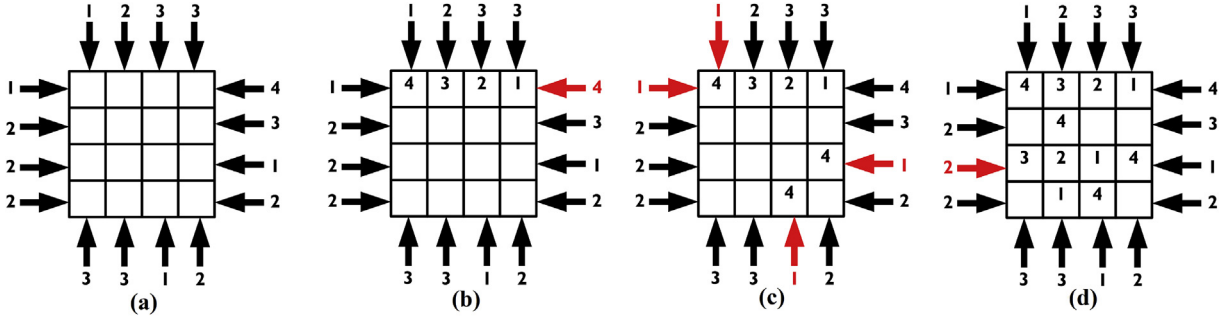

Fig. 9. Illustration of skyscraper puzzle: (a) 4 × 4 grid with clues, (b) fill the row based on the clue 4, (c) fill the row based on the clue 1, and (d) fill the row based on the clue 2.

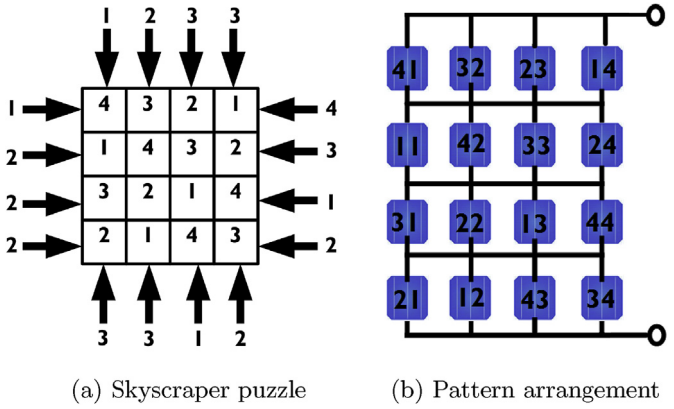

Fig. 10. skyscraper puzzle and pattern arrangement.

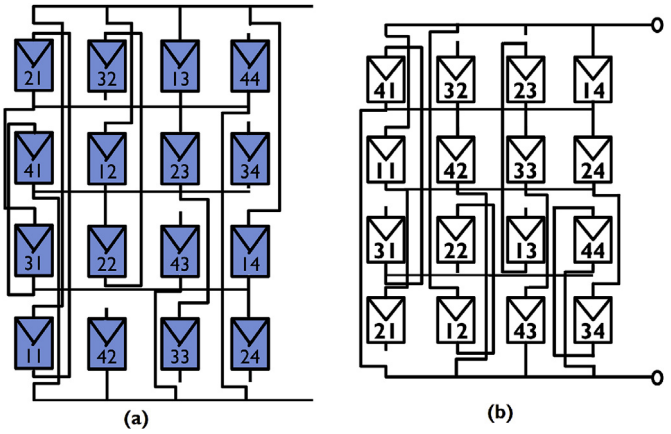

Fig. 11. Physical arrangement: (a) Ken-Ken,(b) Skyscraper.

3.3. Physical relocation

The proposed Ken-Ken and Skyscraper PV array pattern arrangements are shown in Figs. 8(b)&10(b) respectively. In these patterns, the first digit in the box contains a logic number and the second digit referred to a column. The main aim of this approach is to rearrange the PV modules in the TCT array according to proposed arrangements so that the partial shading effects will distribute over the array. In Fig. 11, shows that the PV modules in TCT array are arranged using the proposed manner. This enables to distribute the location shading modules from one place to over the array. Hence, the power generated by the PV array is enhanced for the same shading condition.

3.4. Description of PSCs

In this paper, two regular shading patterns are considered to verify the proposed arrangements; they are referred to as shading pattern-I and shading pattern-II. Each shading pattern is divided into four progressive shading cases such as case-I, case-II, case-III, and case-IV. The irradiance of a shading PV module is 400 W/m^2 and a non-shading PV module is 1000 W/m^2.

3.5. Performance parameters under PSCs

In this paper, five parameters are considered to evaluate the performance of proposed arrangements such as GMPP, V_{GMPP} mismatch losses(%), fill-factor(%) and efficiency(%) on 4×4 array under different shading patterns.

Fill factor.

Fill factor (FF) essentially measures the area of PV module or array. The FF can be determined as,

$$FF(\%) = \frac{Power\ at\ GMPP}{V_{oc}.I_{sc}} \tag{8}$$

Mismatch loss.

Mismatch loss is the difference between the maximum power under uniform irradiance condition (MPP_{uni})and the global maximum power under PSCs ($GMPP_{PSCs}$). Mismatch loss can be determined:

$$ML(\%) = \frac{MPP_{uni} - GMPP_{PSCs}}{GMPP_{PSCs}} \tag{9}$$

Efficiency.

Efficiency is the ratio of available maximum power output to the solar input. Efficiency can be calculate by,

$$Efficiency(\eta) = \frac{Power\ at\ GMPP}{P_{in}} \tag{10}$$

where P_{in} is the solar irradiance falls on the PV array.

4. Results and discussions

This paper proposed the Ken-Ken and Skyscraper PV array arrangements for 4×4 TCT array to enhance maximum power under various shading patterns. Each pattern divided into four shading cases. In each case, the location of GMPP is estimated theoretically for TCT, Magic-square (MS) [13], Latin-square (LS) [14], Ken-Ken and Skyscraper arrangements. The obtained GMPP validated by using Matlab-Simulink model. Also, the proposed arrangements are

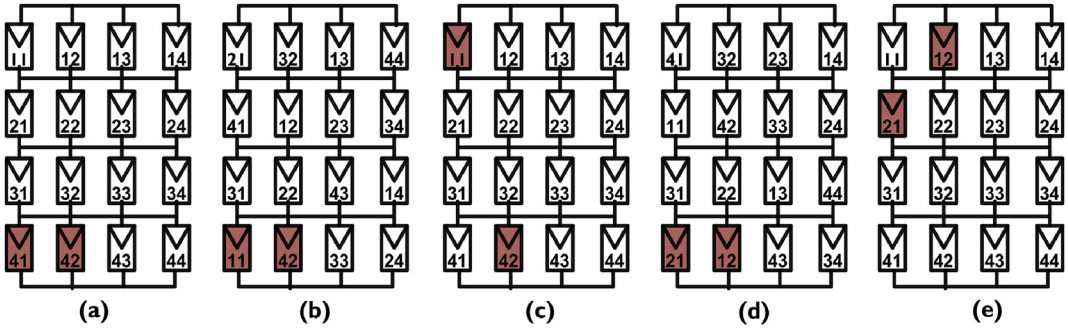

Fig. 12. Shading case-I:(a) TCT arrangement, (b–c) Ken-Ken arrangement and shading dispersion, (d–e) Skyscraper arrangement and shading dispersion.

Table 2
Location of GMPP for TCT, MS [13], LS [14], Ken-Ken and Skyscraper arrangements under shading case-I in pattern-I.

TCT arrangement				Ken-Ken arrangement				Skyscraper arrangement				MS arrangement [13]				LS arrangement [14]			
Row bypassed	current (I_a)	voltage (V_a)	power (P_a)	Row bypassed	currents (I_a)	voltages (V_a)	power(P_a)	Row bypassed	current (I_a)	voltage (V_a)	power (P_a)	Row bypassed	currents (I_a)	voltages (V_a)	power(P_a)	Row bypassed	currents (I_a)	voltages (V_a)	power(P_a)
$Irow_1$	$4I_m$	$3V_m$	$12V_m.I_m$	$Irow_1$	$3.4I_m$	$4V_m$	$13.6V_m.I_m$	$Irow_1$	$3.4I_m$	$4V_m$	$13.6V_m.I_m$	$Irow_1$	$3.4I_m$	$4V_m$	$13.6V_m.I_m$	$Irow_1$	$4I_m$	$2V_m$	$8V_m.I_m$
$Irow_2$	$4I_m$	$3V_m$	$12V_m.I_m$	$Irow_2$	$4I_m$	$2V_m$	$8V_m.I_m$	$Irow_2$	$3.4I_m$	$4V_m$	$13.6V_m.I_m$	$Irow_2$	$4I_m$	$2V_m$	$8V_m.I_m$	$Irow_2$	$4I_m$	$2V_m$	$8V_m.I_m$
$Irow_3$	$4I_m$	$3V_m$	$12V_m.I_m$	$Irow_3$	$4I_m$	$2V_m$	$8V_m.I_m$	$Irow_3$	$4I_m$	$2V_m$	$8V_m.I_m$	$Irow_3$	$4I_m$	$2V_m$	$8V_m.I_m$	$Irow_3$	$3.4I_m$	$4V_m$	$13.6V_m.I_m$
$Irow_4$	$2.8I_m$	$4V_m$	$11.2V_m.I_m$	$Irow_4$	$3.4I_m$	$4V_m$	$13.6V_m.I_m$	$Irow_4$	$4I_m$	$2V_m$	$8V_m.I_m$	$Irow_4$	$3.4I_m$	$4V_m$	$13.6V_m.I_m$	$Irow_4$	$3.4I_m$	$4V_m$	$13.6V_m.I_m$

Similarly, the same procedure is applied to remaining shading cases to find the location of GMPP for PV array arrangements.

continued to compare with SP, BL, and HC PV array configurations by obtaining the GMPP, V_{GMPP}, ML, FF, Efficiency and PLP.

4.1. Performance of PV array arrangements under shading pattern-I

Shading pattern-I, four shading cases are taken into account such as case-I, case-II, case-III and case-IV. In each case, two PV modules is subjected to partial shading in vertically in the first two columns of the array. The location of GMPP for TCT, MS, LS, KK and SS PV array arrangements are calculated theoretically for each case and validated with the Simulink model.

Case-I. In case-I, two PV modules in the last row of the array is subjected to partial shading with various irradiance levels is shown in Fig. 12(a). In this case, the location of GMPP is calculated theoretically for TCT, MS [13], LS [14], Ken-Ken and Skyscraper PV array arrangements as follows,

Location of GMPP for TCT arrangement: The identification of GMPP is by knowing the current across each row of the PV array. So that current generated by the each row is calculated as follows.

In shading case-I, all PV modules in the *row*1 are receiving 1000 W/m^2 irradiance is shown in Fig. 12(a). Therefore, current generated by the *row*1 is,

$$I_{row1} = B_{11}I_{11} + B_{12}I_{12} + B_{13}I_{13} + B_{14}I_{14} \tag{11}$$

$B_{11} = \frac{G_{11}}{G_o} = 1$; where G_{11} is solar irradiance falls on the 11^{th} module in a TCT arrangement and I_{11} is current generated by the module. Assume that current generated by the each module under STC is I_m.

$$I_{row1} = 4 \times I_m \tag{12}$$

All PV modules in *row*2 and *row*3 are receiving uniform irradiance 1000 W/m^2. So that, current generated by the *row*2 is,

$$I_{row2} = I_{row3} = 4I_m \tag{13}$$

In *row*4, two PV modules is receiving 400 W/m^2 irradiance and rest of the PV modules is receiving 1000 W/m^2 irradiance respectively. The current generated by the *row*4,

$$I_{row4} = 2 \times I_m + 0.8I_m \tag{14}$$

Since the current generated by each row is different, there exist multiple peaks in the P—V characteristics. Now to find the location of GMPP is a multiplication of voltage and current of the each row in TCT array. The output current depends on the amount of irradiance falling on the PV modules in a row. However, the voltage is equal for all the rows (by neglecting voltage drop). So the array voltage becomes,

$$V_a = 4 \times V_m \tag{15}$$

Power generated by the PV array,

$$P_a = V_a.I_m = 4V_m.I_m \tag{16}$$

The obtained current, voltage and corresponding power for TCT arrangement is noted in Table 2. The location of GMPP for Ken-Ken and Skyscraper arrangements are calculated as follows.

Location of GMPP for Ken-Ken arrangement: The Ken-Ken arrangement enable to distribute the shading effects over the array under same shading case is shown in Fig. 12(c).

In *row*2 and *row*3, all PV modules is receiving 1000 W/m^2. The current generated by *row*2 and *row*3 is,

$$I_{row2} = I_{row3} = 4 \times I_m \tag{17}$$

In *row*1 and *row*4, one PV module is receiving 400 W/m^2 and

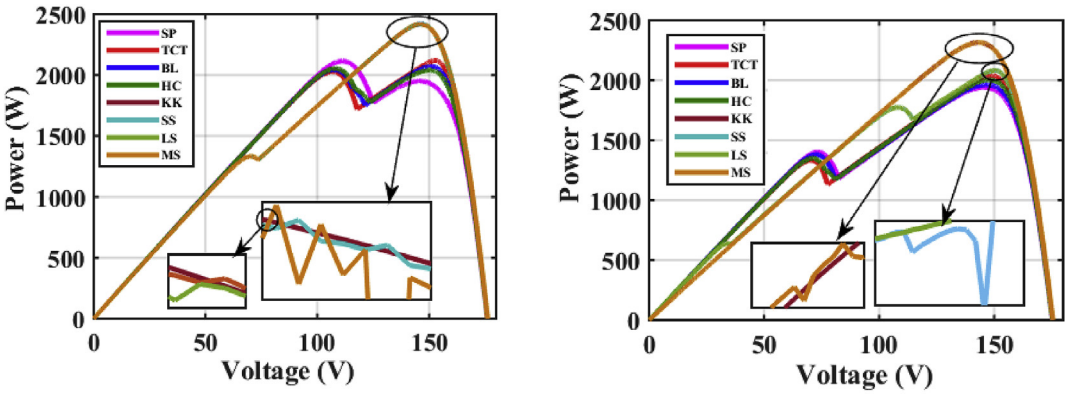

(a) P-V characteristics for case-I (b) P-V characteristics for case-II

Fig. 13. Simulation results for shading pattern-I.

rest of the PV modules is receiving 1000 W/m^2 irradiance. The current generated by *row*1 and *row*4 is,

$$I_{row1} = I_{row4} = 3 \times I_m + 0.4I_m \tag{18}$$

The obtained current, voltage and corresponding power for Ken-Ken arrangement is noted in Table 2. Similarly, the location of GMPP for Skyscraper, magic-square [13] and lain-square [14] arrangements are calculated theoretically and noted in Table 2. From the table, it is recognized that the highest GMPP 13.6 $V_m.I_m$ is produced by the KK, SS, LS and MS arrangements as compared to TCT. Whereas, the theoretical GMPP validated by plotting the simulated P—V characteristics is shown in Fig. 13(a). In addition to this, "SP, BL and HC" PV array configurations also simulated for the same shading case is shown in Fig. 13(a). Under this case, the obtained parameters such as GMPP, V_{GMPP} ML, FF, η and PLP for all configurations is presented in Table 6. From the table, it is understood that the Ken-Ken, Skyscraper, LS and MS arrangements are enhancing the global maximum power by 16.6%, 13.9%, 19.5%, and 22.3% as compared to "SP, TCT, BL, and HC" PV array configurations.

Case-II. In case-II, two PV modules each is subjected to partial shading in the first two columns of the array with various irradiance levels is shown in Fig. 14(a). The location of GMPP is calculated for all arrangements and presented in Table 3. From the table, it is recognized that the highest GMPP 13.6 $V_m.I_m$ is produced by the KK and MS PV array arrangements as compared to TCT, SS and LS arrangements. The GMPP validated by plotting the simulated P—V characteristics is shown in Fig. 13(b). In addition to this, "SP, BL, and HC" PV array configurations also simulated for the same shading case is shown in Fig. 13(b). Under this case, the obtained parameters such as GMPP, V_{GMPP}, ML, FF, η and PLP for all configurations is presented in Table 6. From the table, it is understood that the Ken-Ken and MS arrangements are enhancing the global maximum power by 18.5%, 13.8%, 17.9%, 17.3%, 11.6%, and 11.6% as compared to "SP, TCT, BL, HC, SS and LS" PV array configurations.

Case-III. In case-III, three PV modules each is subjected to partial shading in the first two columns of the array with various irradiance levels is shown in Fig. 16(a). The location of GMPP is calculated for all arrangements and presented in Table 4. From the table, it is recognized that the highest GMPP 11.2 $V_m.I_m$ is produced by the TCT, Ken-Ken, Skyscraper, MS and LS arrangements. The simulated P—V characteristics is shown in Fig. 15(a). In addition to this, "SP, BL, and HC" array configurations also simulated for the same shading case is shown in Fig. 15(a). Under this case, the obtained parameters such as GMPP, V_{GMPP}, ML, FF, η and PLP are presented in Table 6. From the table, it is clearly understood that the Ken-Ken, Skyscraper, LS and MS arrangements are enhancing the global maximum power by 3.8%, 4.5%, 6.2% and 3.8% as compared to "SP, TCT, BL and HC" PV array configurations.

Case-IV. In case-IV, the PV modules in first two columns of the PV array is subjected to partial shading with various irradiance levels is shown in Fig. 17(a). The location of GMPP is calculated for all arrangements and presented in Table 5. From the table, it is recognized that the highest GMPP 11.2 $V_m.I_m$ is produced by the TCT, KK, SS, LS and MS PV array arrangements. The simulated P—V characteristics is shown in Fig. 15(b). In addition to this, "SP, BL, and HC" PV array configurations also simulated for the same shading case is shown in Fig. 15(b). Under this case, the obtained parameters such as GMPP, V_{GMPP}, ML, FF, η and PLP for all configurations is presented in Table 6.From the table, it is understood that the "SP, TCT, BL, HC, Ken-Ken, Skyscraper, LS and MS" arrangements are producing the equal global maximum power.

4.2. Performance of PV array arrangements under shading pattern-II

Shading pattern-II, four shading cases are taken into account such as case-I, case-II, case-III and case-IV. In each case, two PV modules is subjected to partial shading in horizontally in the last two rows of the array. The location of GMPP for TCT, MS, LS, KK and SS PV array arrangements are calculated theoretically for each case and validated with the Simulink model. The performance of PV array arrangements under each shading case is described as follows.

Case-I. In case-I, two PV modules in the first column of the array is subjected to partial shading with various irradiance levels is shown in Fig. 19(a). The location of GMPP is calculated for all arrangements and presented in Table 7. From the table, it is recognized that the highest GMPP 13.6 $V_m.I_m$ is produced by the TCT, KK, SS, LS and MS PV array arrangements. The simulated P—V characteristics is shown in Fig. 18(a). In addition to this, "SP, BL, and HC" PV array configurations also simulated for the same shading case is shown in Fig. 18(a). Under this case, the obtained parameters such as GMPP, V_{GMPP}, ML, FF, η and PLP for all configurations is presented in Table 11. From the table, it is clearly noticed that the TCT, Ken-Ken, Skyscraper, MS and LS arrangements are enhancing the global maximum power by 6.2%, 5.5%, and 6.2% as compared to "SP, BL, and HC" PV array configurations.

Table 3
Location of GMPP for TCT, MS [13], LS [14], Ken-Ken and Skyscraper arrangements under shading case-II in pattern-I.

TCT arrangement				Ken-Ken arrangement				Skyscraper arrangement				MS arrangement [13]				LS arrangement [14]			
Row bypassed	current (I_a)	voltage (V_a)	power (P_a)	Row bypassed	currents (I_a)	voltages (V_a)	power(P_a)	Row bypassed	current (I_a)	voltage (V_a)	power (P_a)	Row bypassed	currents (I_a)	voltages (V_a)	power(P_a)	Row bypassed	currents (I_a)	voltages (V_a)	power(P_a)
$Irow_1$	$4I_m$	$2V_m$	$8V_m.I_m$	$Irow_1$	$3.4I_m$	$4V_m$	$13.6V_m.I_m$	$Irow_1$	$3.4I_m$	$3V_m$	$10.2V_m.I_m$	$Irow_1$	$3.4I_m$	$4V_m$	$13.6V_m.I_m$	$Irow_1$	$4I_m$	V_m	$4V_m.I_m$
$Irow_2$	$4I_m$	$2V_m$	$8V_m.I_m$	$Irow_2$	$3.4I_m$	$4V_m$	$13.6V_m.I_m$	$Irow_2$	$2.8I_m$	$4V_m$	$11.2V_m.I_m$	$Irow_2$	$3.4I_m$	$4V_m$	$13.6V_m.I_m$	$Irow_2$	$2.8I_m$	$4V_m$	$11.2V_m.I_m$
$Irow_3$	$2.8I_m$	$4V_m$	$11.2V_m.I_m$	$Irow_3$	$3.4I_m$	$4V_m$	$13.6V_m.I_m$	$Irow_3$	$3.4I_m$	$3V_m$	$10.2 V_m.I_m$	$Irow_3$	$3.4I_m$	$4V_m$	$13.6V_m.I_m$	$Irow_3$	$2.8I_m$	$4V_m$	$11.2V_m.I_m$
$Irow_4$	$2.8I_m$	$4V_m$	$11.2V_m.I_m$	$Irow_4$	$3.4I_m$	$4V_m$	$13.6V_m.I_m$	$Irow_4$	$4I_m$	V_m	$4V_m.I_m$	$Irow_4$	$3.4I_m$	$4V_m$	$13.6V_m.I_m$	$Irow_4$	$3.4I_m$	$3V_m$	$10.2V_m.I_m$

Table 4
Location of GMPP for TCT, MS [13], LS [14], Ken-Ken and Skyscraper arrangements under shading case-III in pattern-I.

TCT arrangement				Ken-Ken arrangement				Skyscraper arrangement				MS arrangement [13]				LS arrangement [14]			
Row bypassed	current (I_a)	voltage (V_a)	power (P_a)	Row bypassed	currents (I_a)	voltages (V_a)	power(P_a)	Row bypassed	current (I_a)	voltage (V_a)	power (P_a)	Row bypassed	currents (I_a)	voltages (V_a)	power(P_a)	Row bypassed	currents (I_a)	voltages (V_a)	power(P_a)
$Irow_1$	$4I_m$	V_m	$4V_m.I_m$	$Irow_1$	$2.8I_m$	$4V_m$	$11.2V_m.I_m$	$Irow_1$	$2.8I_m$	$4V_m$	$11.2V_m.I_m$	$Irow_1$	$3.4I_m$	$2V_m$	$6.8 V_m.I_m$	$Irow_1$	$3.4I_m$	$2V_m$	$6.8 V_m.I_m$
$Irow_2$	$2.8I_m$	$4V_m$	$11.2V_m.I_m$	$Irow_2$	$3.4I_m$	$2V_m$	$6.8V_m.I_m$	$Irow_2$	$2.8I_m$	$4V_m$	$11.2V_m.I_m$	$Irow_2$	$2.88I_m$	$4V_m$	$11.2V_m.I_m$	$Irow_2$	$2.8I_m$	$4V_m$	$11.2V_m.I_m$
$Irow_3$	$2.8I_m$	$4V_m$	$11.2V_m.I_m$	$Irow_3$	$3.4I_m$	$2V_m$	$6.8V_m.I_m$	$Irow_3$	$3.4I_m$	$2V_m$	$6.8 V_m.I_m$	$Irow_3$	$2.8I_m$	$4V_m$	$11.2V_m.I_m$	$Irow_3$	$2.8I_m$	$4V_m$	$11.2V_m.I_m$
$Irow_4$	$2.8I_m$	$4V_m$	$11.2V_m.I_m$	$Irow_4$	$2.8I_m$	$4V_m$	$11.2V_m.I_m$	$Irow_4$	$3.4I_m$	$2V_m$	$6.8 V_m.I_m$	$Irow_4$	$3.4I_m$	$2V_m$	$6.8 V_m.I_m$	$Irow_4$	$3.4I_m$	$2V_m$	$6.8 V_m.I_m$

Table 5
Location of GMPP for TCT, MS [13], LS [14], Ken-Ken and Skyscraper arrangements under shading case-IV in pattern-I.

TCT arrangement				Ken-Ken arrangement				Skyscraper arrangement				MS arrangement [13]				LS arrangement [14]			
Row bypassed	current (I_a)	voltage (V_a)	power (P_a)	Row bypassed	currents (I_a)	voltages (V_a)	power(P_a)	Row bypassed	current (I_a)	voltage (V_a)	power (P_a)	Row bypassed	currents (I_a)	voltages (V_a)	power(P_a)	Row bypassed	currents (I_a)	voltages (V_a)	power(P_a)
$Irow_1$	$2.8I_m$	$4V_m$	$11.2V_m.I_m$	$Irow_1$	$2.8I_m$	$4V_m$	$11.2V_m.I_m$	$Irow_1$	$2.8I_m$	$4V_m$	$11.2V_m.I_m$	$Irow_1$	$2.8I_m$	$4V_m$	$11.2V_m.I_m$	$Irow_1$	$2.8I_m$	$4V_m$	$11.2V_m.I_m$
$Irow_2$	$2.8I_m$	$4V_m$	$11.2V_m.I_m$	$Irow_2$	$2.8I_m$	$4V_m$	$11.2V_m.I_m$	$Irow_2$	$2.8I_m$	$4V_m$	$11.2V_m.I_m$	$Irow_2$	$2.8I_m$	$4V_m$	$11.2V_m.I_m$	$Irow_2$	$2.8I_m$	$4V_m$	$11.2V_m.I_m$
$Irow_3$	$2.8I_m$	$4V_m$	$11.2V_m.I_m$	$Irow_3$	$2.8I_m$	$4V_m$	$11.2V_m.I_m$	$Irow_3$	$2.8I_m$	$4V_m$	$11.2V_m.I_m$	$Irow_3$	$2.8I_m$	$4V_m$	$11.2V_m.I_m$	$Irow_3$	$2.8I_m$	$4V_m$	$11.2V_m.I_m$
$Irow_4$	$2.8I_m$	$4V_m$	$11.2V_m.I_m$	$Irow_4$	$2.8I_m$	$4V_m$	$11.2V_m.I_m$	$Irow_4$	$2.8I_m$	$4V_m$	$11.2V_m.I_m$	$Irow_4$	$2.8I_m$	$4V_m$	$11.2V_m.I_m$	$Irow_4$	$2.8I_m$	$4V_m$	$11.2V_m.I_m$

Table 6
GMPP, V_{GMPP} ML, FF, η and PLP for various PV array configurations in shading pattern-I.

Configurations	CASE I						CASE II						CASE III						CASE IV					
	GMPP (W)	V_{GMPP} (V)	M.Loss	FF	η	PLP	GMPP	V_{GMPP}	M.Loss	FF	η	PLP	GMPP	V_{GMPP}	M.Loss	FF	η	PLP	GMPP	V_{GMPP}	M.Loss	FF	η	PLP
SP	2100	118	620	57.10	10.2	1	1940	150	780	52.7	9.47	1	1950	146	770	53.02	9.52	1	1820	145	900	49.4	8.89	0
TCT	2150	160	570	58.4	10.5	1	2020	156	700	54.9	9.87	1	1960	148	760	53.2	9.57	1	1820	145	900	49.4	8.89	0
BL	2050	156	670	55.7	10.01	2	1950	151	770	53.02	9.52	1	1990	148	730	54.1	9.72	1	1820	145	900	49.4	8.89	0
HC	2000	156	720	54.3	9.77	2	1960	150	760	53.2	9.57	1	1950	146	770	53.02	9.52	1	1820	145	900	49.4	8.89	0
KK	2450	148	270	66.6	11.9	1	2300	141	420	62.5	11.2	1	2010	148	710	54.65	9.82	1	1820	145	900	49.4	8.89	0
SS	2450	148	270	66.6	11.9	1	2060	150	660	56.01	10.06	2	2010	148	710	54.6	9.82	1	1820	145	900	49.4	8.89	0
LS	2450	148	270	66.6	11.9	1	2060	150	660	56.01	10.06	1	2010	148	710	54.6	9.82	1	1820	145	900	49.4	8.89	0
MS	2450	148	270	66.6	11.9	1	2300	141	660	56.01	11.2	2	2010	148	710	54.6	9.82	1	1820	145	900	49.4	8.89	0

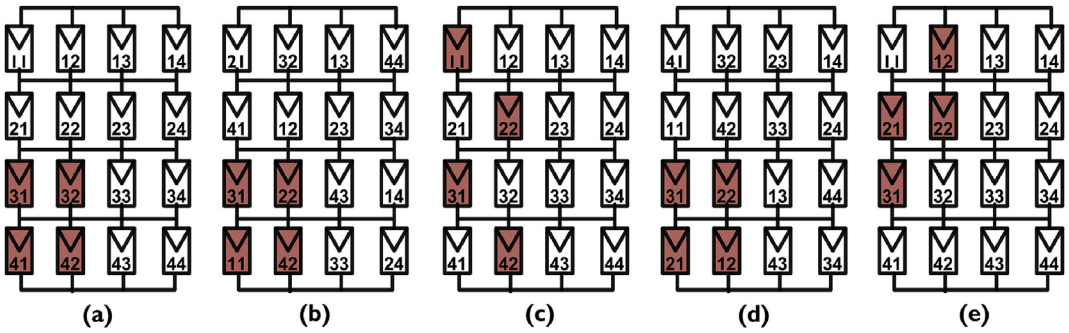

Fig. 14. Shading case-II:(a) TCT arrangement, (b–c) KK arrangement and shading dispersion, (d–e) SS arrangement and shading dispersion.

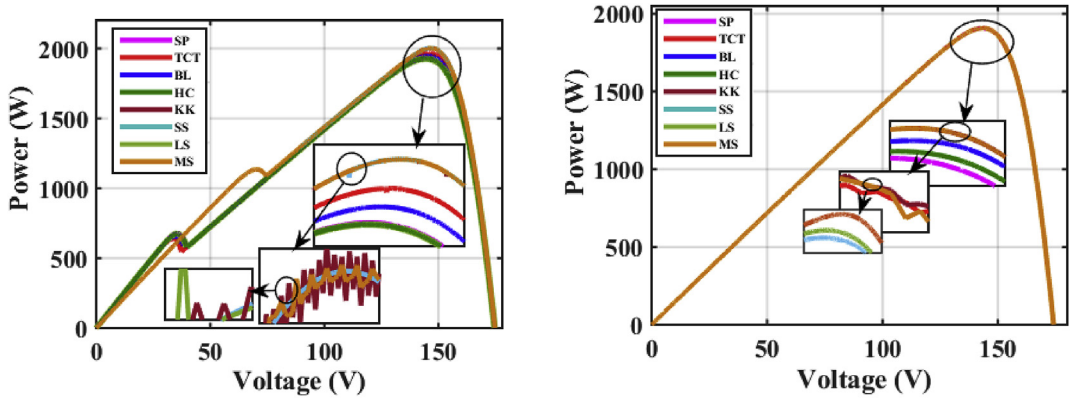

(a) P-V characteristics for case-III (b) P-V characteristics for case-IV

Fig. 15. Simulation results for shading pattern-I.

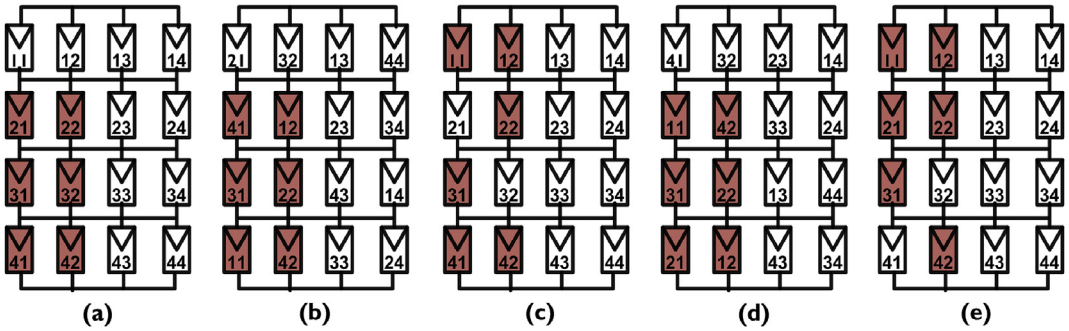

Fig. 16. Shading case-III:(a) TCT arrangement, (b–c) Ken-Ken arrangement and shading dispersion, (d–e) Skyscraper arrangement and shading dispersion.

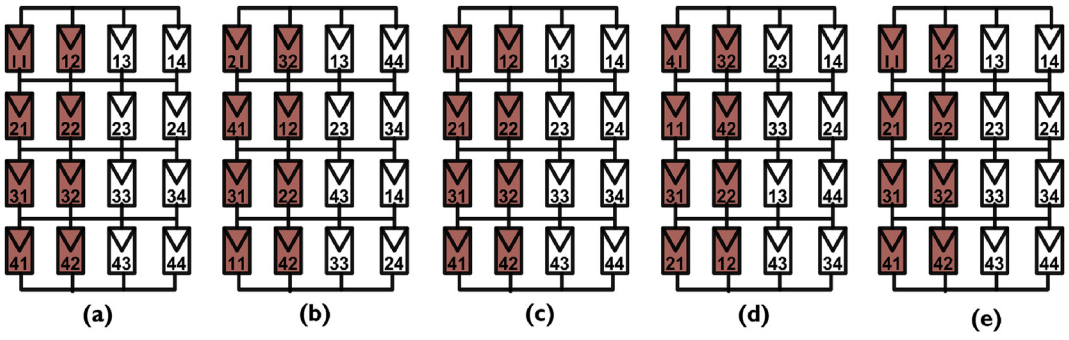

Fig. 17. Shading case-IV:(a) TCT arrangement, (b–c) Ken-Ken arrangement and shading dispersion, (d–e) Skyscraper arrangement and shading dispersion.

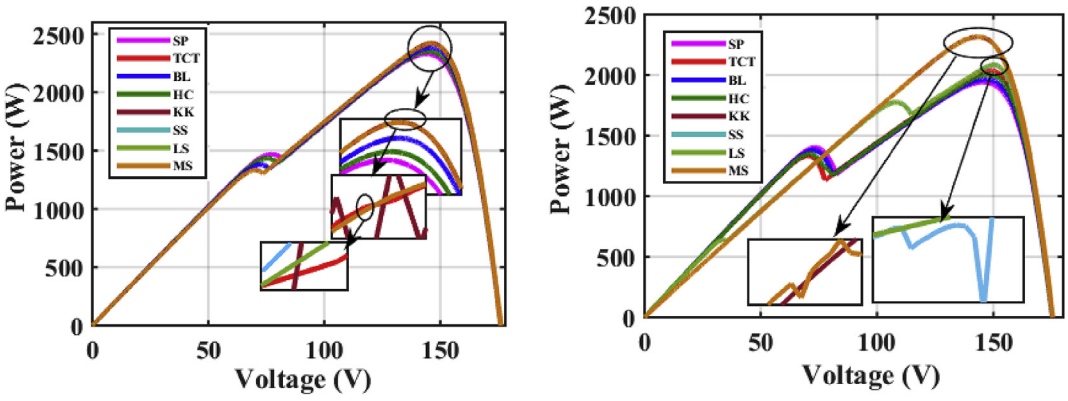

(a) P-V characteristics for case-I (b) P-V characteristics for case-II

Fig. 18. Simulation results for shading pattern-II.

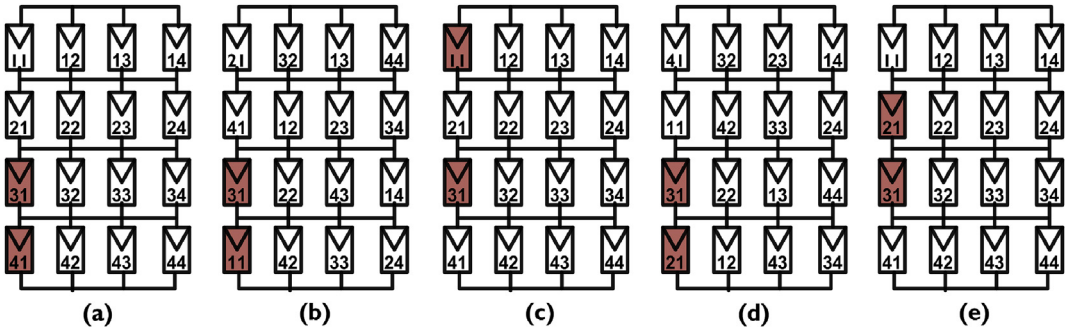

Fig. 19. Shading case-a:(a) TCT arrangement, (b–c) Ken-Ken arrangement and shading dispersion, (d–e) Skyscraper arrangement and shading dispersion.

Case-II. In case-II, two PV modules each is subjected to partial shading in the last two rows of the array with different irradiances is shown in Fig. 21(a). The location of GMPP is calculated for all arrangements and presented in Table 8. From the table, it is recognized that the highest GMPP 13.6 $V_m.I_m$ is produced by the Ken-Ken and MS arrangements as compared to TCT, Skyscraper and LS PV array arrangements. The simulated P–V characteristics is shown in Fig. 18(b). In addition to this, "SP, BL, and HC PV array configurations also simulated for the same shading case is shown in Fig. 18(b). Under this case, the obtained parameters such as GMPP, V_{GMPP}, ML, FF, η and PLP for all configurations are presented in Table 11. From the table, it is clearly noticed that the Ken-Ken and MS arrangements are enhancing the global maximum power by 18.5%, 13.8%, 17.9%, 17.3%, 11.6%, and 11.6% as compared to "SP, TCT, BL, HC, Skyscraper and LS" PV array configurations.

Case-III. In case-III, three PV modules each is subjected to partial shading in the last two rows of the array with different irradiances is shown in Fig. 22(a). The location of GMPP is calculated for all arrangements and presented in Table 9. From the table, it is recognized that the highest GMPP 13.6 $V_m.I_m$ is produced by the Ken-Ken, Skyscraper, MS and LS arrangements as compared to TCT arrangement. The simulated P–V characteristics is shown in Fig. 20(a). In addition to this, "SP, BL, and HC" PV array configurations also simulated for the same shading case is shown in Fig. 20(a). Under this case, the obtained parameters such as GMPP, V_{GMPP}, ML, FF, η and PLP for all configurations is presented in Table 11. From the table, it is clearly noticed that the Ken-Ken, Skyscraper, MS and LS arrangements are enhancing the global maximum power by 29.5%, 26.2%, 29.1%, and 28.7% as compared to "SP, TCT, BL and HC" PV array configurations.

Case-IV. In case-IV, last two rows of the array is subjected to partial shading with different irradiances is shown in Fig. 23(a). The location of GMPP is calculated for all arrangements and presented in Table 10. From the table, it is recognized that the highest GMPP 11.2 $V_m.I_m$ is produced by the Ken-Ken, Skyscraper, MS and LS arrangements as compared to TCT arrangement. The simulated P–V characteristics is shown in Fig. 20(b). In addition to this, "SP, BL, and HC" PV array configurations also simulated for the same shading case is shown in Fig. 20(b). Under this case, the obtained parameters such as GMPP, V_{GMPP}, ML, FF, η and PLP for all configurations is presented in Table 11. From the table, it is clearly noticed that the Ken-Ken, Skyscraper, MS and LS arrangements are enhancing the global maximum power by 46.9% as compared to "SP, TCT, BL and HC" PV array configurations.

In summary, the performance of Ken-Ken and Skyscraper arrangements are investigated with SP, TCT, BL, HC, MS [13] and LS [14] PV array configurations under different shading cases. The above-mentioned result shows that the proposed arrangements are producing the highest global maximum power when compared to other configurations under most shading cases. Also, the performance of Ken-Ken and Skyscraper PV array arrangements is very close to the MS and LS arrangement and far than the "SP, TCT, BL, and HC" configurations under most shading cases. Therefore, this paper extended to study the performance of Ken-Ken, Skyscraper, MS and LS PV array arrangements under various shading conditions (i.e., shading pattern-III) and temperatures (i.e., shading pattern-IV).

Table 7
Location of GMPP for TCT, MS [13], LS [14], Ken-Ken and Skyscraper arrangements under shading case-I in pattern-II.

TCT arrangement				Ken-Ken arrangement				Skyscraper arrangement				MS arrangement [13]				LS arrangement [14]			
Row bypassed	current (I_a)	voltage (V_a)	power (P_a)	Row bypassed	currents (I_a)	voltages (V_a)	power(P_a)	Row bypassed	current (I_a)	voltage (V_a)	power (P_a)	Row bypassed	currents (I_a)	voltages (V_a)	power(P_a)	Row bypassed	currents (I_a)	voltages (V_a)	power(P_a)
$Irow_1$	$4I_m$	$2V_m$	$8V_m.I_m$	$Irow_1$	$3.4I_m$	$4V_m$	$13.6V_m.I_m$	$Irow_1$	$4I_m$	$2V_m$	$8V_m.I_m$	$Irow_1$	$4I_m$	$2V_m$	$8V_m.I_m$	$Irow_1$	$4I_m$	$2V_m$	$8V_m.I_m$
$Irow_2$	$4I_m$	$2V_m$	$8V_m.I_m$	$Irow_2$	$4I_m$	$2V_m$	$8V_m.I_m$	$Irow_2$	$3.4I_m$	$4V_m$	$13.6V_m.I_m$	$Irow_2$	$3.4I_m$	$4V_m$	$13.6V_m.I_m$	$Irow_2$	$4I_m$	$2V_m$	$8V_m.I_m$
$Irow_3$	$3.4I_m$	$4V_m$	$13.6V_m.I_m$	$Irow_3$	$3.4I_m$	$4V_m$	$13.6V_m.I_m$	$Irow_3$	$3.4I_m$	$4V_m$	$13.6V_m.I_m$	$Irow_3$	$4I_m$	$2V_m$	$8V_m.I_m$	$Irow_3$	$3.4I_m$	$4V_m$	$13.6V_m.I_m$
$Irow_4$	$3.4I_m$	$4V_m$	$13.6V_m.I_m$	$Irow_4$	$4I_m$	$2V_m$	$8V_m.I_m$	$Irow_4$	$4I_m$	$2V_m$	$8V_m.I_m$	$Irow_4$	$3.4I_m$	$4V_m$	$13.6V_m.I_m$	$Irow_4$	$3.4I_m$	$4V_m$	$13.6V_m.I_m$

Table 8
Location of GMPP for TCT, MS [13], LS [14], Ken-Ken and Skyscraper arrangements under shading case-II in pattern-II.

TCT arrangement				Ken-Ken arrangement				Skyscraper arrangement				MS arrangement [13]				LS arrangement [14]			
Row bypassed	current (I_a)	voltage (V_a)	power (P_a)	Row bypassed	currents (I_a)	voltages (V_a)	power(P_a)	Row bypassed	current (I_a)	voltage (V_a)	power (P_a)	Row bypassed	currents (I_a)	voltages (V_a)	power(P_a)	Row bypassed	currents (I_a)	voltages (V_a)	power(P_a)
$Irow_1$	$4I_m$	$2V_m$	$8V_m.I_m$	$Irow_1$	$3.4I_m$	$4V_m$	$13.6V_m.I_m$	$Irow_1$	$3.4I_m$	$3V_m$	$10.2V_m.I_m$	$Irow_1$	$3.4I_m$	$4V_m$	$13.6V_m.I_m$	$Irow_1$	$4I_m$	V_m	$4V_m.I_m$
$Irow_2$	$4I_m$	$2V_m$	$8V_m.I_m$	$Irow_2$	$3.4I_m$	$4V_m$	$13.6V_m.I_m$	$Irow_2$	$2.8I_m$	$4V_m$	$11.2V_m.I_m$	$Irow_2$	$3.4I_m$	$4V_m$	$13.6V_m.I_m$	$Irow_2$	$2.8I_m$	$4V_m$	$11.2V_m.I_m$
$Irow_3$	$2.8I_m$	$4V_m$	$11.2V_m.I_m$	$Irow_3$	$3.4I_m$	$4V_m$	$13.6V_m.I_m$	$Irow_3$	$3.4I_m$	$3V_m$	10.2 $V_m.I_m$	$Irow_3$	$3.4I_m$	$4V_m$	$13.6V_m.I_m$	$Irow_3$	$2.8I_m$	$4V_m$	$11.2V_m.I_m$
$Irow_4$	$2.8I_m$	$4V_m$	$11.2V_m.I_m$	$Irow_4$	$3.4I_m$	$4V_m$	$13.6V_m.I_m$	$Irow_4$	$4I_m$	V_m	$4V_m.I_m$	$Irow_4$	$3.4I_m$	$4V_m$	$13.6V_m.I_m$	$Irow_4$	$3.4I_m$	$3V_m$	$10.2V_m.I_m$

Table 9
Location of GMPP for TCT, MS [13], LS [14], Ken-Ken and Skyscraper arrangements under shading case-III in pattern-II.

TCT arrangement				Ken-Ken arrangement				Skyscraper arrangement				MS arrangement [13]				LS arrangement [14]			
Row bypassed	current (I_a)	voltage (V_a)	power (P_a)	Row bypassed	currents (I_a)	voltages (V_a)	power(P_a)	Row bypassed	current (I_a)	voltage (V_a)	power (P_a)	Row bypassed	currents (I_a)	voltages (V_a)	power(P_a)	Row bypassed	currents (I_a)	voltages (V_a)	power(P_a)
$Irow_1$	$4I_m$	$2V_m$	$8V_m.I_m$	$Irow_1$	$3.4I_m$	$2V_m$	$6.8V_m.I_m$	$Irow_1$	$3.4I_m$	$3V_m$	$10.2V_m.I_m$	$Irow_1$	$3.4I_m$	$2V_m$	$6.8V_m.I_m$	$Irow_1$	$2.8I_m$	$4V_m$	$11.2V_m.I_m$
$Irow_2$	$4I_m$	$2V_m$	$8V_m.I_m$	$Irow_2$	$3.4I_m$	$2V_m$	$6.8V_m.I_m$	$Irow_2$	$2.8I_m$	$4V_m$	$11.2V_m.I_m$	$Irow_2$	$3.4I_m$	$2V_m$	$6.8V_m.I_m$	$Irow_2$	$2.8I_m$	$4V_m$	$11.2V_m.I_m$
$Irow_3$	$2.2I_m$	$4V_m$	$8.8V_m.I_m$	$Irow_3$	$3.4I_m$	$4V_m$	$13.6V_m.I_m$	$Irow_3$	$3.4I_m$	$3V_m$	10.2 $V_m.I_m$	$Irow_3$	$2.8I_m$	$4V_m$	$11.2V_m.I_m$	$Irow_3$	$3.4I_m$	$2V_m$	$6.8V_m.I_m$
$Irow_4$	$2.2I_m$	$4V_m$	$8.8V_m.I_m$	$Irow_4$	$3.4I_m$	$4V_m$	$13.6V_m.I_m$	$Irow_4$	$4I_m$	V_m	$4V_m.I_m$	$Irow_4$	$2.8I_m$	$4V_m$	$11.2V_m.I_m$	$Irow_4$	$3.4I_m$	$6.8V_m$	$6.8V_m.I_m$

Table 10
Location of GMPP for TCT, MS [13], LS [14], Ken-Ken and Skyscraper arrangements under shading case-IV in pattern-II.

TCT arrangement				Ken-Ken arrangement				Skyscraper arrangement				MS arrangement [13]				LS arrangement [14]			
Row bypassed	current (I_a)	voltage (V_a)	power (P_a)	Row bypassed	currents (I_a)	voltages (V_a)	power(P_a)	Row bypassed	current (I_a)	voltage (V_a)	power (P_a)	Row bypassed	currents (I_a)	voltages (V_a)	power(P_a)	Row bypassed	currents (I_a)	voltages (V_a)	power(P_a)
$Irow_1$	$4I_m$	$2V_m$	$8V_m.I_m$	$Irow_1$	$2.8I_m$	$4V_m$	$11.2V_m.I_m$	$Irow_1$	$2.8I_m$	$4V_m$	$11.2V_m.I_m$	$Irow_1$	$2.8I_m$	$4V_m$	$11.2V_m.I_m$	$Irow_1$	$2.8I_m$	$4V_m$	$11.2V_m.I_m$
$Irow_2$	$4I_m$	$2V_m$	$8V_m.I_m$	$Irow_2$	$2.8I_m$	$4V_m$	$11.2V_m.I_m$	$Irow_2$	$2.8I_m$	$4V_m$	$11.2V_m.I_m$	$Irow_2$	$2.8I_m$	$4V_m$	$11.2V_m.I_m$	$Irow_2$	$2.8I_m$	$4V_m$	$11.2V_m.I_m$
$Irow_3$	$1.6I_m$	$4V_m$	$6.4V_m.I_m$	$Irow_3$	$2.8I_m$	$4V_m$	$11.2V_m.I_m$	$Irow_3$	$2.8I_m$	$4V_m$	$11.2V_m.I_m$	$Irow_3$	$2.8I_m$	$4V_m$	$11.2V_m.I_m$	$Irow_3$	$2.8I_m$	$4V_m$	$11.2V_m.I_m$
$Irow_4$	$1.6I_m$	$4V_m$	$6.4V_m.I_m$	$Irow_4$	$2.8I_m$	$4V_m$	$11.2V_m.I_m$	$Irow_4$	$2.8I_m$	$4V_m$	$11.2V_m.I_m$	$Irow_4$	$2.8I_m$	$4V_m$	$11.2V_m.I_m$	$Irow_4$	$2.8I_m$	$4V_m$	$11.2V_m.I_m$

Table 11
GMPP, V_{GMPP} ML, FF, η and PLP for various PV array configurations in shading pattern-II.

Configurations	CASE I						CASE II						CASE III						CASE IV					
	GMPP (W)	V_{GMPP} (V)	M.Loss	FF	η	PLP	GMPP	V_{GMPP}	M.Loss	FF	η	PLP	GMPP	V_{GMPP}	M.Loss	FF	η	PLP	GMPP	V_{GMPP}	M.Loss	FF	η	PLP
SP	2250	146	470	61.1	10.9	1	1940	150	780	52.7	9.47	1	1550	152	1170	42.14	7.57	1	1280	68	1440	34.8	6.25	1
TCT	2400	148	320	65.2	11.72	1	2020	156	700	54.9	9.87	1	1590	157	1130	43.2	7.76	2	1280	68	1440	34.8	6.25	1
BL	2260	146	460	61.4	11.04	1	1950	151	770	53.02	9.52	1	1555	153	1165	42.2	7.59	1	1280	68	1440	34.8	6.25	1
HC	2254	146	466	61.2	11.01	1	1960	150	760	53.2	9.57	1	1560	153	1160	42.4	7.62	1	1280	68	1440	34.8	6.25	1
KK	2400	148	320	65.2	11.72	1	2300	141	420	62.5	11.2	1	2008	148	712	54.69	9.82	1	1880	145	840	51.1	9.18	0
SS	2400	148	320	65.2	11.72	1	2060	150	660	56.01	10.06	2	2008	148	712	54.69	9.82	1	1880	145	840	51.1	9.18	0
LS	2400	148	320	65.2	11.72	1	2060	150	660	56.01	10.06	1	2008	148	712	54.69	9.82	1	1880	145	840	51.1	9.18	0
MS	2400	148	320	65.2	11.72	1	2300	141	660	56.01	11.2	2	2008	148	712	54.69	9.82	1	1880	145	840	51.1	9.18	0

4.3. Performance of PV array arrangements under shading pattern-III

In shading pattern-III, four shading cases are taken into account such as case-I, case-II, case-III and case-IV. In each case, the location of GMPP for MS, LS, KK and SS PV array arrangements are calculated theoretically and validated with the Simulink model.

Case-I. In case-I, bottom most right corner 2×2 sub-array is subjected to partial shading with various irradiance levels is shown in Fig. 24(a). The location of GMPP is calculated for all arrangements and presented in Table 12. From the table, it is recognized that both MS and Ken-Ken arrangements are producing the highest GMPP 13.2 $V_m.I_m$ as compared to LS and SS arrangements.The simulated P–V characteristics is shown in Fig. 26(a). Under this case, the obtained parameters such as GMPP, V_{GMPP}, ML, FF, η and PLP are presented in Table 16. From the Table, it is noticed that the Ken-Ken and MS arrangements are enhancing the global maximum power by 7.9% compared to LS, and SS PV array configurations.

Case-II. In case-I, bottom most left corner 2×2 sub-array is subjected to partial shading with various irradiance levels is shown in Fig. 25(a). The location of GMPP is calculated for all arrangements and presented in Table 13. From the table, it recognized that the Ken-Ken and Skyscraper arrangements are producing the highest GMPP 13.6 $V_m.I_m$ as compared to MS and LS arrangements. The simulated P–V characteristics is shown in Fig. 26(b). Under this case, the obtained parameters such as GMPP, V_{GMPP}, ML, FF, η and PLP are presented in Table 16. From the Table, it is noticed that the Ken-Ken and Skyscraper arrangements are enhancing the global maximum power by 13.2% as compared to LS and MS PV array configurations.

Case-III. In case-III, top-most right corner 2×2 sub-array is subjected to partial shading with various irradiance levels is shown in Fig. 27(a). The location of GMPP is calculated for all arrangements and presented in Table 14. From the table, it is recognized that the Skyscraper and Ken-Ken arrangement are producing the highest GMPP 12 $V_m.I_m$ as compared to MS and LS arrangements. The simulated P–V characteristics is shown in Fig. 29(a). Under this case, the obtained parameters such as GMPP, V_{GMPP}, ML, FF, η and PLP are presented in Table 16. From the Table, it is noticed that the Skyscraper and Ken-Ken arrangements are enhancing the global maximum power by 8.4% compared to LS and MS PV array configurations.

Case-IV. In case-IV, top-most left corner 2×2 sub-array is subjected to partial shading with various irradiance levels is shown in Fig. 28(a). The location of GMPP is calculated for all arrangements and presented in Table 15. From the table, it is recognized that both Skyscraper and Ken-Ken arrangements are producing the highest GMPP 12.8 $V_m.I_m$ as compared to MS and LS arrangements. The simulated P–V characteristics is shown in Fig. 29(b). Under this case, the obtained parameters such as GMPP, V_{GMPP}, ML, FF, η and PLP are presented in Table 16. From the Table, it is noticed that the Ken-Ken and Skyscraper arrangements are enhancing the global maximum power by 9.5% as compared to LS and MS PV array configurations.

4.4. Effect of temperature on MS, LS, Skyscraper and Ken-Ken PV array arrangements

The temperature typically affects the output voltage of an array. In this paper, various temperature levels are considered such as 25°C, 30°C and 35°C (adding ±5 to the ambient temperature) for showing the effect on output power in 4×4 MS, LS, SS and KK

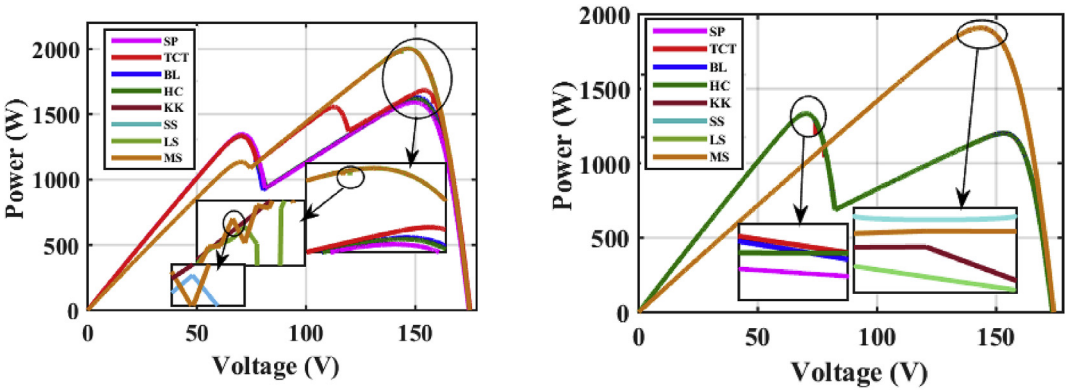

(a) P-V characteristics for case-III (b) P-V characteristics for case-IV

Fig. 20. Simulation results for shading pattern-II.

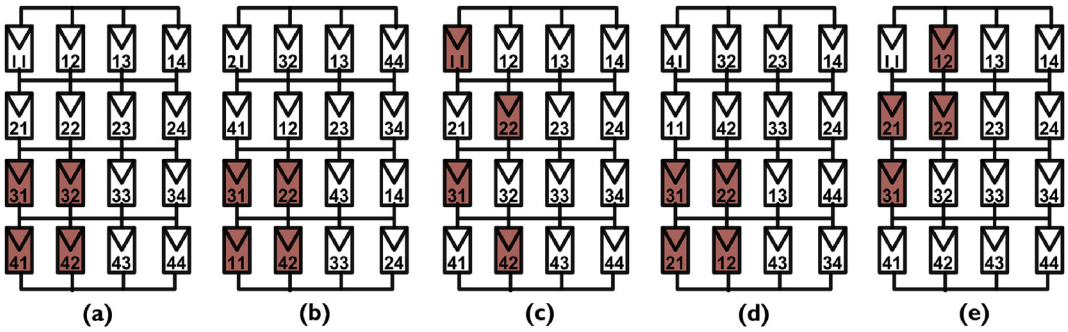

Fig. 21. Shading case-a:(a) TCT arrangement, (b–c) Ken-Ken arrangement and shading dispersion, (d–e) Skyscraper arrangement and shading dispersion.

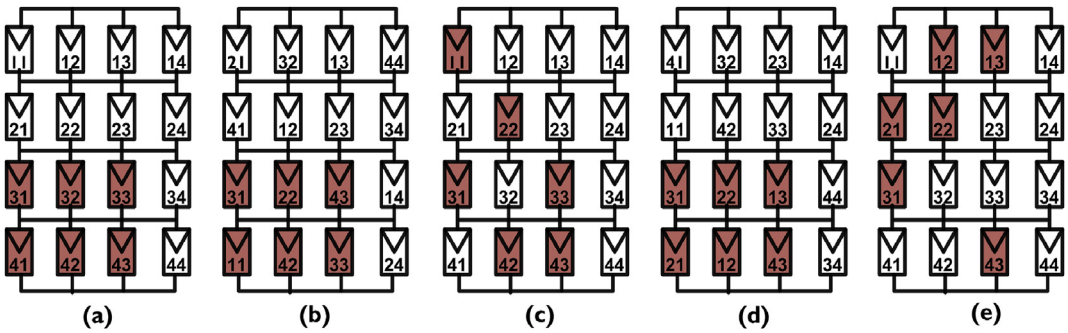

Fig. 22. Shading case-a:(a) TCT arrangement, (b–c) Ken-Ken arrangement and shading dispersion, (d–e) Skyscraper arrangement and shading dispersion.

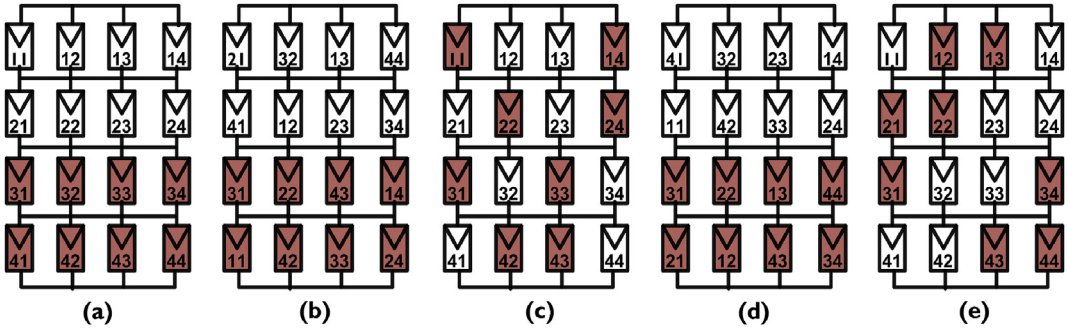

Fig. 23. Shading case-a:(a) TCT arrangement, (b–c) Ken-Ken arrangement and shading dispersion, (d–e) Skyscraper arrangement and shading dispersion.

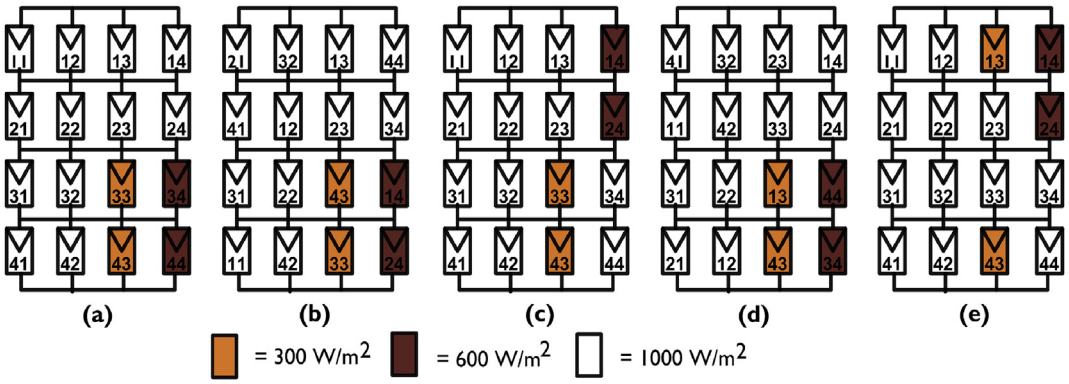

Fig. 24. Shading case-a:(a) TCT arrangement, (b–c) Ken-Ken arrangement and shading dispersion and (d–e) Skyscraper arrangement and shading dispersion.

Table 12
Location of GMPP for Ken-Ken, Skyscraper, MS [13] and LS [14] arrangements under shading case-I in pattern-III.

Skyscraper arrangement				Ken-Ken arrangement				MS arrangement [13]				LS arrangement [14]			
Row bypassed	current (I_a)	voltage (V_a)	power (P_a)	Row bypassed	currents (I_a)	voltages (V_a)	power (P_a)	Row bypassed	current (I_a)	voltage (V_a)	power (P_a)	Row bypassed	currents (I_a)	voltages (V_a)	power (P_a)
$Irow_1$	$3.3I_m$	$3V_m$	$9.9V_m.I_m$	$Irow_1$	$3.6I_m$	$2V_m$	$7.2V_m.I_m$	$Irow_1$	$3.6I_m$	$2V_m$	$7.2V_m.I_m$	$Irow_1$	$2.6I_m$	$4V_m$	$10.4V_m.I_m$
$Irow_2$	$4I_m$	V_m	$4V_m.I_m$	$Irow_2$	$3.6I_m$	$2V_m$	$7.2V_m.I_m$	$Irow_2$	$3.6I_m$	$2V_m$	$7.2V_m.I_m$	$Irow_2$	$3.3I_m$	$3V_m$	$9.9V_m.I_m$
$Irow_3$	$3.6I_m$	$2V_m$	$7.2V_m.I_m$	$Irow_3$	$3.3I_m$	$4V_m$	$13.2V_m.I_m$	$Irow_3$	$3.3I_m$	$4V_m$	$13.2V_m.I_m$	$Irow_3$	$4I_m$	V_m	$4V_m.I_m$
$Irow_4$	$2.9I_m$	$4V_m$	$11.6V_m.I_m$	$Irow_4$	$3.3I_m$	$4V_m$	$13.2V_m.I_m$	$Irow_4$	$3.3I_m$	$4V_m$	$13.2V_m.I_m$	$Irow_4$	$3.3I_m$	$3V_m$	$9.9V_m.I_m$

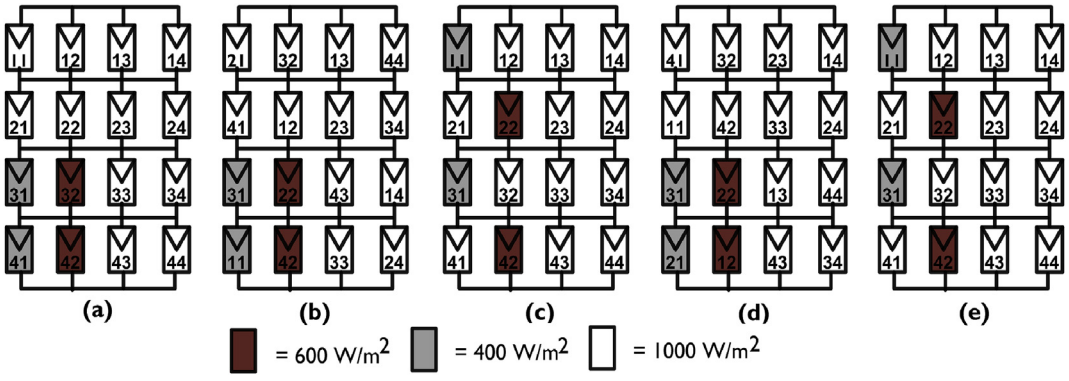

Fig. 25. Shading case-a:(a) TCT arrangement, (b–c) Ken-Ken arrangement and shading dispersion and (d–e) Skyscraper arrangement and shading dispersion.

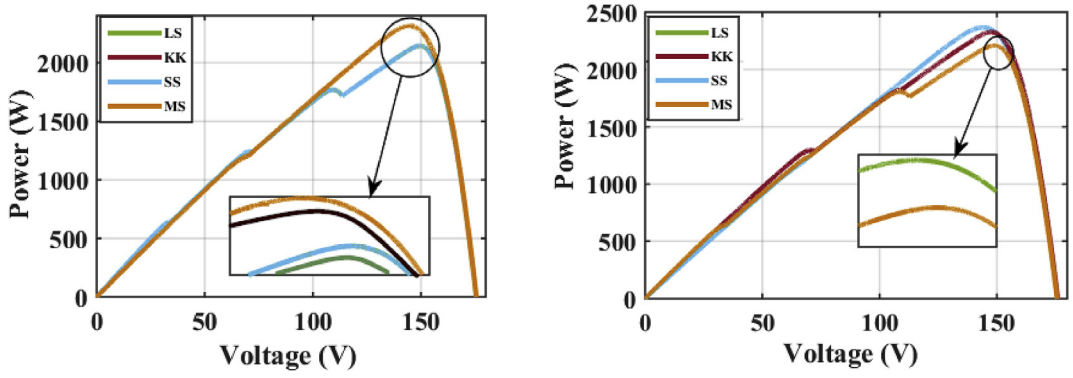

(a) P-V characteristics for case-I

(b) P-V characteristics for case-II

Fig. 26. Simulation results for shading pattern-III.

Table 13
Location of GMPP for TCT, MS [13], LS [14] and Ken-Ken arrangements under shading case-II in pattern-III.

Skyscraper arrangement				Ken-Ken arrangement				MS arrangement [13]				LS arrangement [14]			
Row bypassed	current (I_a)	voltage (V_a)	power (P_a)	Row bypassed	currents (I_a)	voltages (V_a)	power(P_a)	Row bypassed	current (I_a)	voltage (V_a)	power (P_a)	Row bypassed	currents (I_a)	voltages (V_a)	power(P_a)
$Irow_1$	$3.6I_m$	$2V_m$	$7.2V_m.I_m$	$Irow_1$	$3.4I_m$	$4V_m$	$13.6V_m.I_m$	$Irow_1$	$3.6I_m$	$2V_m$	$7.2V_m.I_m$	$Irow_1$	$4I_m$	V_m	$4V_m.I_m$
$Irow_2$	$3.4I_m$	$4V_m$	$13.6V_m.I_m$	$Irow_2$	$3.6I_m$	$2V_m$	$7.2V_m.I_m$	$Irow_2$	$3.6I_m$	$2V_m$	$7.2V_m.I_m$	$Irow_2$	$3.6I_m$	$2V_m$	$7.2V_m.I_m$
$Irow_3$	$3.6I_m$	$3V_m$	$10.8V_m.I_m$	$Irow_3$	$3.4I_m$	$4V_m$	$13.6V_m.I_m$	$Irow_3$	$3.2I_m$	$4V_m$	$12.8V_m.I_m$	$Irow_3$	$3I_m$	$4V_m$	$12V_m.I_m$
$Irow_4$	$4I_m$	V_m	$4V_m.I_m$	$Irow_4$	$3.6I_m$	$2V_m$	$7.2V_m.I_m$	$Irow_4$	$3.2I_m$	$4V_m$	$12.8V_m.I_m$	$Irow_4$	$3.4I_m$	$3V_m$	$10.2V_m.I_m$

Table 14
Location of GMPP for TCT, MS [13], LS [14] and Ken-Ken arrangements under shading case-III in pattern-III.

Skyscraper arrangement				Ken-Ken arrangement				MS arrangement [13]				LS arrangement [14]			
Row bypassed	current (I_a)	voltage (V_a)	power (P_a)	Row bypassed	currents (I_a)	voltages (V_a)	power(P_a)	Row bypassed	current (I_a)	voltage (V_a)	power (P_a)	Row bypassed	currents (I_a)	voltages (V_a)	power(P_a)
$Irow_1$	$3.1I_m$	$3V_m$	$9.1V_m.I_m$	$Irow_1$	$3.7I_m$	$2V_m$	$7.4V_m.I_m$	$Irow_1$	$3.7I_m$	$2V_m$	$7.4V_m.I_m$	$Irow_1$	$4I_m$	V_m	$4V_m.I_m$
$Irow_2$	$3I_m$	$4V_m$	$12V_m.I_m$	$Irow_2$	$3.7I_m$	$2V_m$	$7.4V_m.I_m$	$Irow_2$	$3.7I_m$	$2V_m$	$7.4V_m.I_m$	$Irow_2$	$3.1I_m$	$3V_m$	$9.3V_m.I_m$
$Irow_3$	$3.7I_m$	$2V_m$	$7.4V_m.I_m$	$Irow_3$	$3.1I_m$	$3V_m$	$9.3V_m.I_m$	$Irow_3$	$2.8I_m$	$4V_m$	$11.2V_m.I_m$	$Irow_3$	$2.8I_m$	$4V_m$	$11.2V_m.I_m$
$Irow_4$	$4I_m$	V_m	$4V_m.I_m$	$Irow_4$	$3I_m$	$4V_m$	$12V_m.I_m$	$Irow_4$	$2.8I_m$	$4V_m$	$11.2V_m.I_m$	$Irow_4$	$3.7I_m$	$2V_m$	$7.4V_m.I_m$

Table 15
Location of GMPP for TCT, MS [13], LS [14] and Ken-Ken arrangements under shading case-IV in pattern-III.

Skyscraper arrangement				Ken-Ken arrangement				MS arrangement [13]				LS arrangement [14]			
Row bypassed	current (I_a)	voltage (V_a)	power (P_a)	Row bypassed	currents (I_a)	voltages (V_a)	power(P_a)	Row bypassed	current (I_a)	voltage (V_a)	power (P_a)	Row bypassed	currents (I_a)	voltages (V_a)	power(P_a)
$Irow_1$	$3.2I_m$	$4V_m$	$12.8V_m.I_m$	$Irow_1$	$3.5I_m$	$2V_m$	$7V_m.I_m$	$Irow_1$	$3I_m$	$4V_m$	$12V_m.I_m$	$Irow_1$	$2.7I_m$	$4V_m$	$10.8V_m.I_m$
$Irow_2$	$4I_m$	V_m	$4V_m.I_m$	$Irow_2$	$3.2I_m$	$4V_m$	$12.8V_m.I_m$	$Irow_2$	$3I_m$	$4V_m$	$12V_m.I_m$	$Irow_2$	$3.2I_m$	$3V_m$	$9.6V_m.I_m$
$Irow_3$	$3.5I_m$	$2V_m$	$7V_m.I_m$	$Irow_3$	$3.5I_m$	$2V_m$	$7V_m.I_m$	$Irow_3$	$3.5I_m$	$2V_m$	$7V_m.I_m$	$Irow_3$	$4I_m$	V_m	$4V_m.I_m$
$Irow_4$	$3.4I_m$	$3V_m$	$10.2V_m.I_m$	$Irow_4$	$3.2I_m$	$4V_m$	$12.8V_m.I_m$	$Irow_4$	$3.5I_m$	$2V_m$	$7V_m.I_m$	$Irow_4$	$3.5I_m$	$2V_m$	$7V_m.I_m$

Table 16
GMPP, V_{GMPP}, ML, FF, η and PLP for various PV array configurations in shading pattern-III.

Configurations	CASE I						CASE II						CASE III						CASE IV					
	GMPP (W)	V_{GMPP} (V)	M.Loss	FF	η	PLP	GMPP	V_{GMPP}	M.Loss	FF	η	PLP	GMPP	V_{GMPP}	M.Loss	FF	η	PLP	GMPP	V_{GMPP}	M.Loss	FF	η	PLP
KK	2250	148	470	61.1	10.9	1	2390	142	330	64.9	11.6	1	2190	148	530	59.5	10.7	1	2200	146	520	59.8	10.75	2
SS	2090	151	630	56.8	10.21	3	2400	147	320	65.2	11.7	0	2190	148	530	59.5	10.7	1	2190	151	530	59.5	10.7	1
LS	2090	151	630	56.8	10.21	3	2120	151	600	57.6	10.35	2	2020	152	700	54.9	9.87	2	2008	153	712	54.6	9.81	2
MS	2250	148	470	61.1	10.9	1	2120	151	600	57.6	10.35	2	2020	152	700	54.9	9.87	2	2008	153	712	54.6	9.81	2

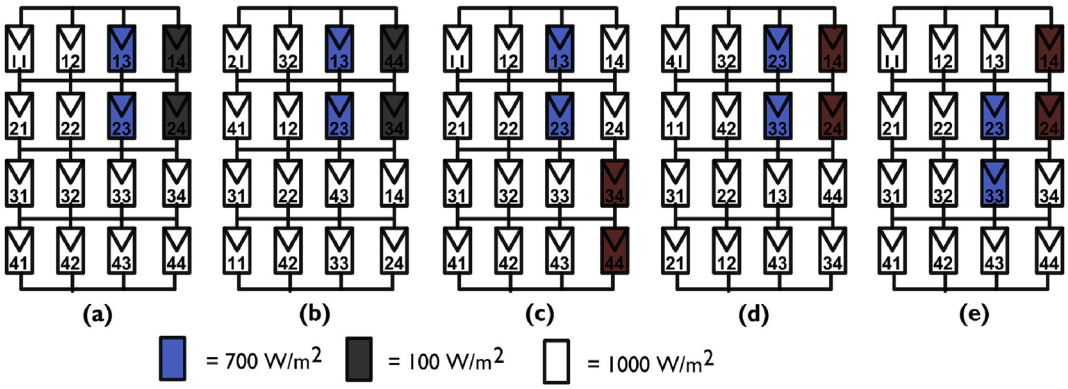

Fig. 27. Shading case-a:(a) TCT arrangement, (b–c) Ken-Ken arrangement and shading dispersion and (d–e) Skyscraper arrangement and shading dispersion.

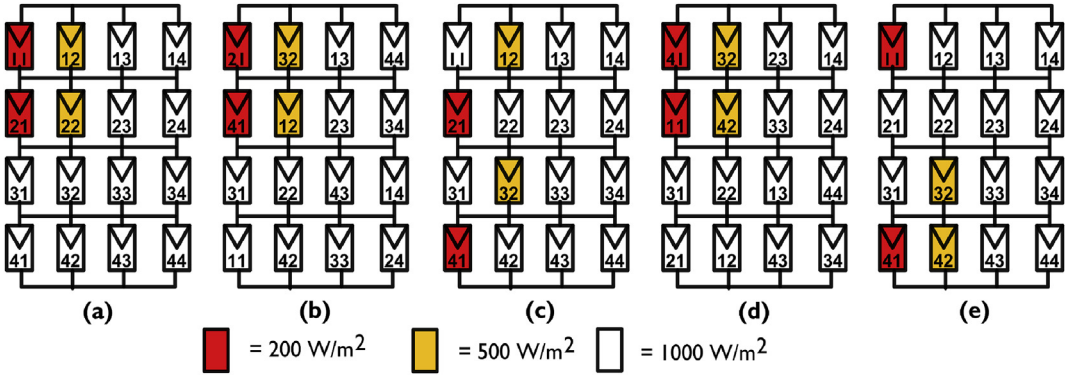

Fig. 28. Shading case-a:(a) TCT arrangement, (b–c) Ken-Ken arrangement and shading dispersion (d–e) Skyscraper arrangement and shading dispersion.

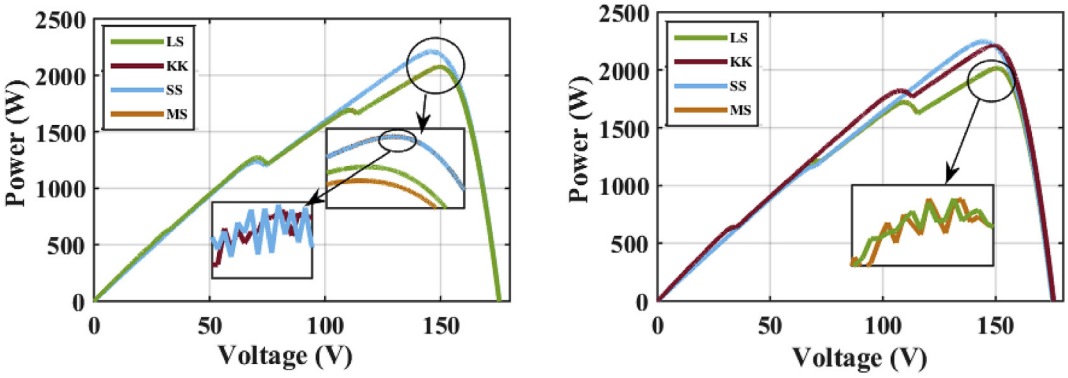

(a) I-V characteristics for case-III

(b) P-V characteristics for case-IV

Fig. 29. Simulation results for shading pattern-III.

arrangements under shading cases I-IV of the shading pattern-IV as shown in Fig. 30. In each shading case, the P–V characteristics is plotted for all configurations by varying the temperature levels, which are shown in Figs. 31–38. Further, the global maximum power is obtained for all arrangements, which is presented in Table 17. From the table, it is noticed that the Ken-Ken and Skyscraper arrangements are producing the highest maximum power which is equal to the MS and far than that of LS.

4.5. Comparison between various reconfiguration schemes

In this section, various existing reconfiguration schemes are compared in terms of maximum power under shading pattern-III. In Ref. [19], reconfiguration approach is presented based on dynamically altering the connection layout of modules in PSCs. However, this technique needs a sensors, switching matrix, and the separate optimization algorithm to perform the experiment. In Refs. [13,14], the magic-square and latin-square pattern arrangements are developed to distribute shading effect over the array. In this approach, the PV modules are physically shifting without altering the electrical connections. However, it doesn't require any switches and sensors but, it needs a pattern that can be distribute shading effects uniformly. The drawback of this technique is that the PV modules connections remain the same for the first column

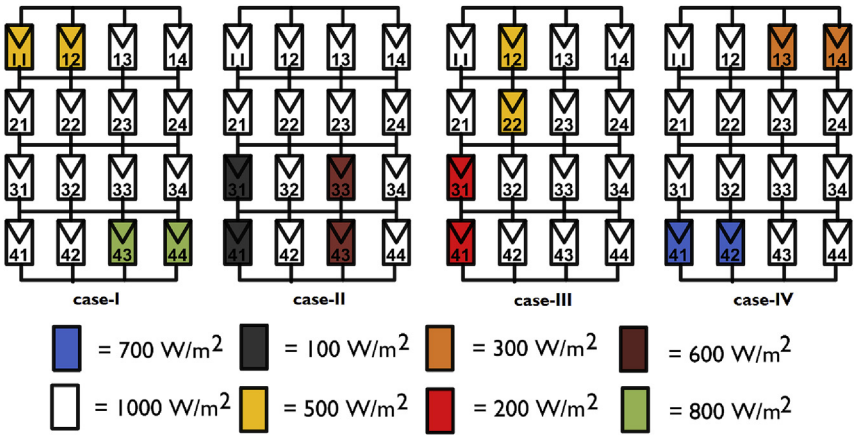

Fig. 30. Shading pattern-IV for TCT PV array arrangement.

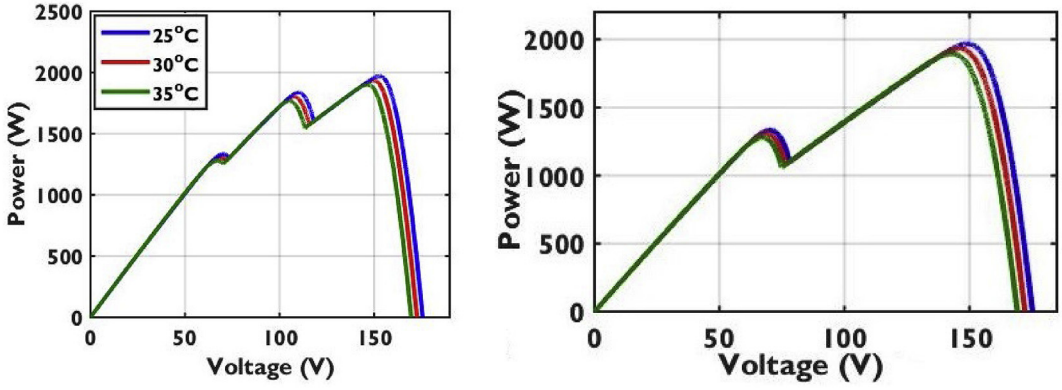

(a) P-V characteristics for MS (b) P-V characteristics for LS

Fig. 31. Simulation results for MS and LS in shading case-I.

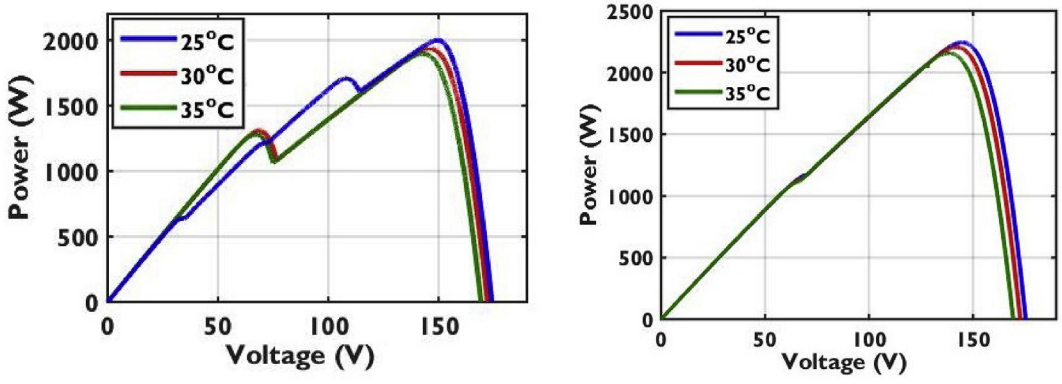

(a) P-V characteristics for SS (b) P-V characteristics for KK

Fig. 32. Simulation results for SS and KK in shading case-I.

of the array. In case of vertical shadings, the PV modules may not be able to distribute the shading effects.

In this work, the Ken-Ken and Skyscraper arrangements are proposed to distribute PSCs and increase maximum power output. The proposed schemes shows superior performance on reduction in mismatch losses when it compared to Refs. [13,14] but, the wiring losses are slightly higher when compare to Ref. [19] under most shading conditions. Table 18, shows the power output of various reconfiguration schemes under shading pattern-III. The power difference between the proposed arrangements and [19] is minimal. However, this improvement is achieved by cause of expensive components such as voltage and current sensors, electronic switches and other parameters. This power difference is invisible if the cost-effective analysis discovered. In addition to this, the better conclusion for the best reconfiguration scheme out of various methods, the wheel chart has prepared as shown in Fig. 39,

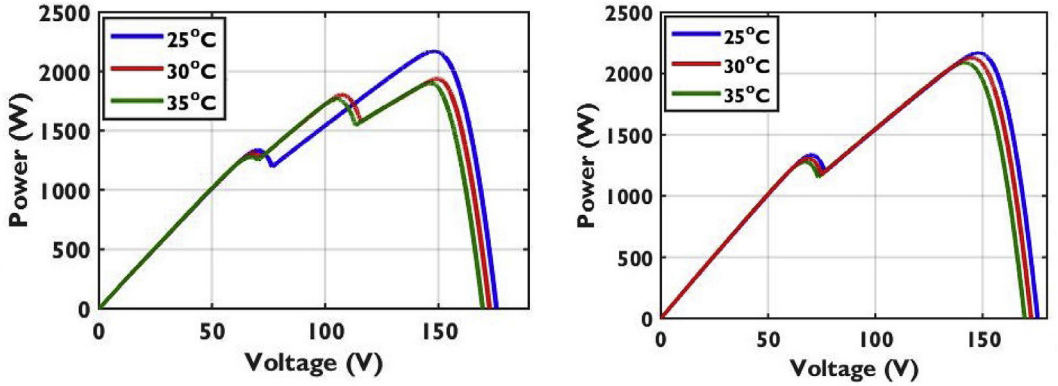

(a) P-V characteristics for MS (b) P-V characteristics for LS

Fig. 33. Simulation results for MS and LS in shading case-II.

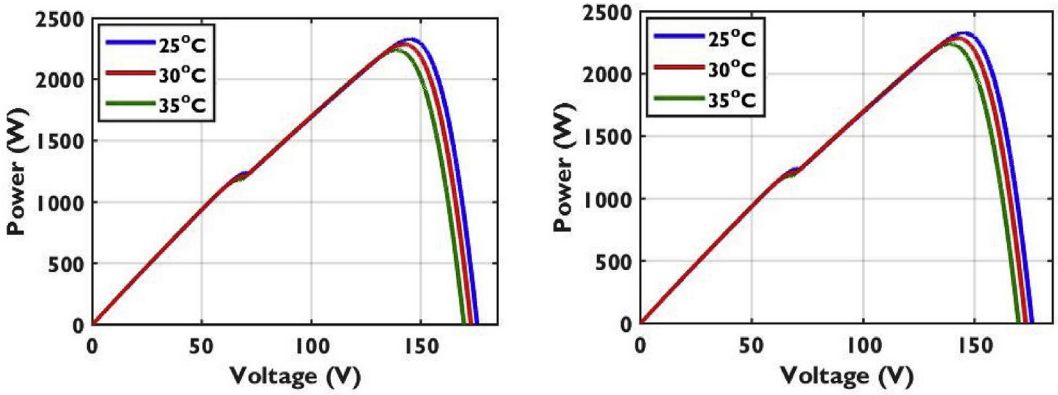

(a) P-V characteristics for SS (b) P-V characteristics for KK

Fig. 34. Simulation results for SS and KK in shading case-II.

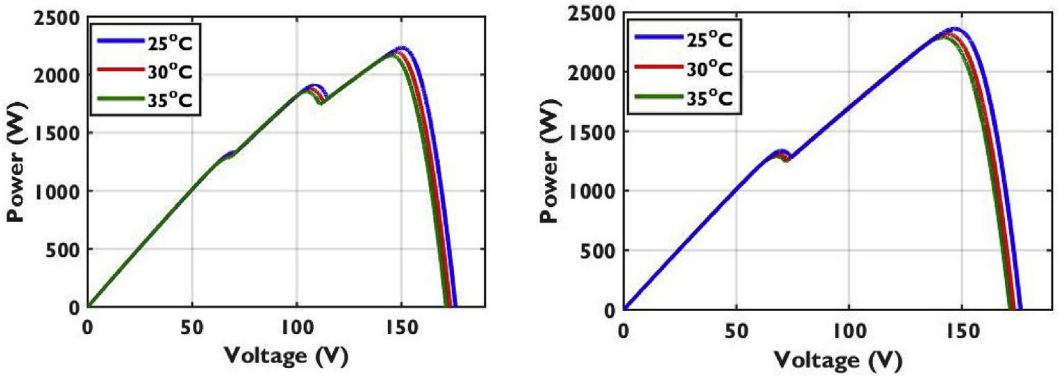

(a) P-V characteristics for MS (b) P-V characteristics for LS

Fig. 35. Simulation results for MS and LS in shading case-III.

for considering several parameters such as required sensors, number of switches, parameters acquired, wiring complexity and algorithm complexity. This wheel chart can be understood in the following way; the chart covers an inner diameter of the wheel is the most favorable method with the higher recommendations. While the chart covers the outer diameter has less adaptability to reconfiguration scheme.

4.6. Extension of large PV arrays

The formulation of proposed Ken-Ken and Skyscraper PV array arrangements are based on the simple logic algorithm. This algorithm can also formulate the large array levels $m \times n$ (i.e., either symmetrical or non-symmetrical), with the constraints of without repeating the numbers in row or column. The overall work performed in this paper is represented in a flow chart is shown in Fig. 40.

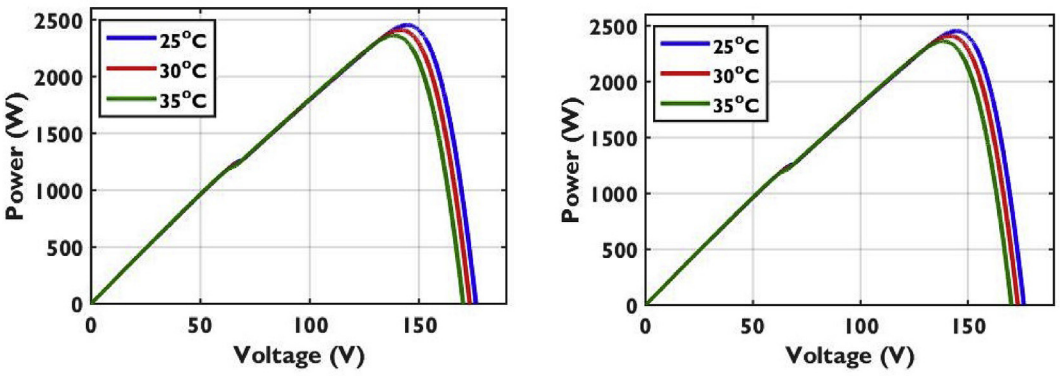

(a) P-V characteristics for SS (b) P-V characteristics for KK

Fig. 36. Simulation results for SS and KK in shading case-III.

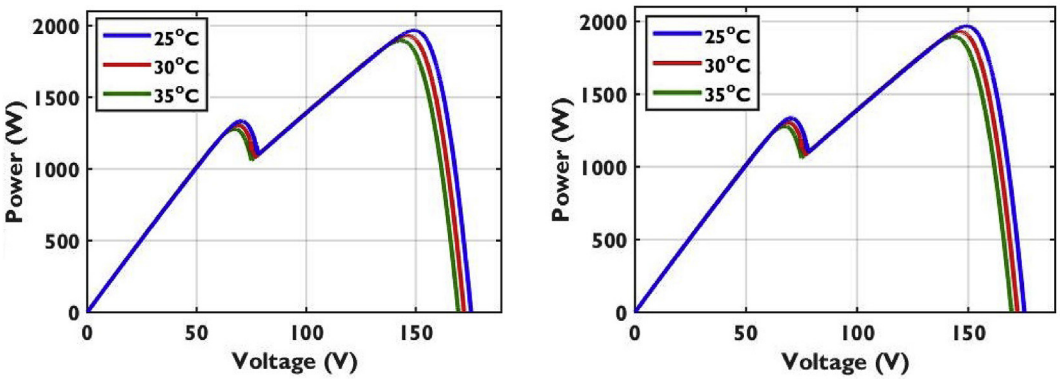

(a) P-V characteristics for MS (b) P-V characteristics for LS

Fig. 37. Simulation results for MS and LS in shading case-IV.

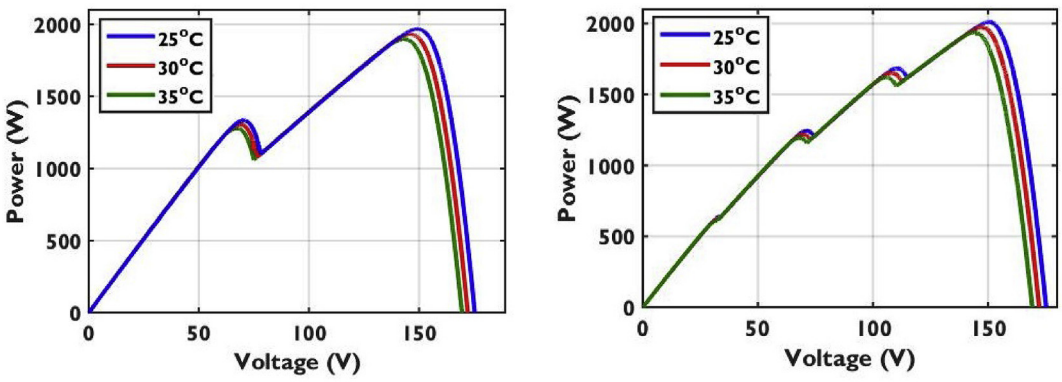

(a) P-V characteristics for SS (b) P-V characteristics for KK

Fig. 38. Simulation results for SS and KK in shading case-IV.

Table 17
GMPP of MS, LS, Skyscraper and Ken-Ken PV array arrangements for various temperatures under shading cases I-V in pattern-IV.

Configurations	case I			case II			case III			case IV		
	25°C	30°C	35°C	25°C	30°C	35°C	25°C	30°C	35°C	25°C	30°C	35°C
MS	1990	1950	1920	2200	1990	1970	2130	2100	2080	1980	1950	1890
LS	1998	1970	1910	2240	2220	2190	2280	2220	2190	1990	1960	1920
Skyscraper	2010	1980	1910	2280	2160	2080	2280	2160	2080	1980	1950	1910
KK	2180	2150	2100	2280	2220	2190	2280	2220	2190	2010	1990	1970

Table 18
Variation in power output for reconfiguration schemes under shading pattern-III.

PV arrangement scheme	case-I	case-II	case-III	case-IV
Parlak et al. [19].	2390	2415	2200	2200
Magic-Square [13]	2250	2120	2020	2008
Latin-Square [14]	2090	2120	2020	2008
Proposed Ken-Ken	2250	2390	2190	2200
Proposed Skyscraper	2090	2400	2190	2200

5. Conclusion

In this paper, the following studies have been reviewed;

- This paper proposed novel reconfiguration schemes followed by Ken-Ken and Skyscraper for 4×4 TCT array to enhance global maximum power under partial shadings. Further, the performance of arrangements are investigated with the existing array configurations such as SP, TCT, BL, HC, MS and LS under various shading patterns using MATLAB-SIMULINK.
- In shading pattern-I & II, the performance of Ken-Ken and Skyscraper PV array arrangement is very close to the MS and LS, far than that of SP, TCT, BL and HC configurations.
- In shading pattern-III, the performance of Ken-Ken and Skyscraper PV array arrangements is better than the MS and LS under most shading cases.
- The overall conclusion of this paper made of two main observations; (i) Ken-Ken and Skyscraper arrangements are enhancing the overall performance as compared to SP, TCT, BL and HC under all shading cases. (ii) The proposed arrangements are also displaying superior performance which is equal or more than that of MS and LS arrangements under most shading cases.

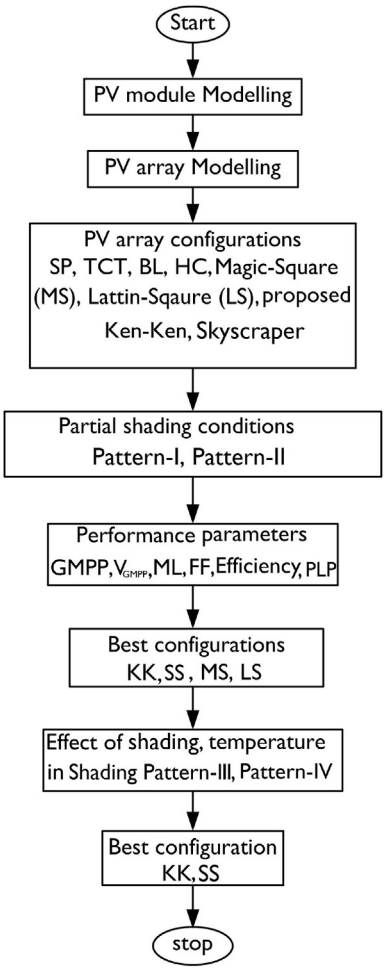

Fig. 40. Flow chart: process of the work done in this paper.

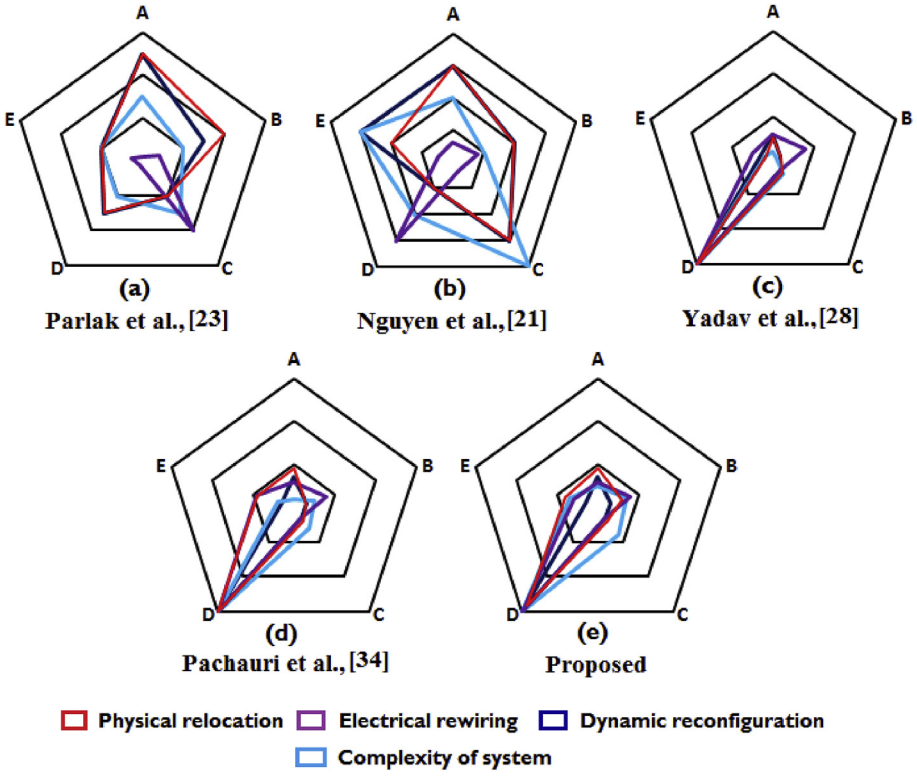

Fig. 39. Wheel chart for reconfiguration schemes: A-required number of sensors, B-number of switches, C-parameters acquired, D-wiring complexity and E-algorithm complexity.

Conflicts of interest

With this note we would like to submit our manuscript, titled "Enhancement of maximum power output through reconfiguration techniques under Non-uniform irradiance conditions", for consideration as a Research article for Energy Journal.

This manuscript has not been published and is not under consideration for publication elsewhere. Thank you very much for your consideration. We don't have any conflict of interest with any other papers. This article doesn't have any funding support and also no relation with industries as well.

Appendix A. Supplementary data

Supplementary data to this article can be found online at https://doi.org/10.1016/j.energy.2019.115917.

References

[1] Al-Dousari Ali, Al-Nassar Waleed, Al-Hemoud Ali, Alsaleh Abeer, Ramadan Ashraf, Al-Dousari Noor, Ahmed Modi. Solar and wind energy: challenges and solutions in desert regions. Energy 2019;176:184–94.

[2] Belhachat Faiza, Larbes Cherif. Comprehensive review on global maximum power point tracking techniques for pv systems subjected to partial shading conditions. Sol Energy 2019;183:476–500.

[3] Du Bolun, Yang Ruizhen, He Yunze, Wang Feng, Huang Shoudao. Nondestructive inspection, testing and evaluation for si-based, thin film and multi-junction solar cells: an overview. Renew Sustain Energy Rev 2017;78:1117–51.

[4] Wang Yaw-Juen, Hsu Po-Chun. An investigation on partial shading of pv modules with different connection configurations of pv cells. Energy 2011;36(5):3069–78.

[5] Gautam NK, Kaushika ND. Network analysis of fault-tolerant solar photovoltaic arrays. Sol Energy Mater Sol Cells 2001;69(1):25–42.

[6] Bingöl Okan, Özkaya Burçin. Analysis and comparison of different pv array configurations under partial shading conditions. Sol Energy 2018;160:336–43.

[7] Sai Krishna G, Moger Tukaram. Improved sudoku reconfiguration technique for total-cross-tied pv array to enhance maximum power under partial shading conditions. Renew Sustain Energy Rev 2019;109:333–48.

[8] Bana Sangram, Saini RP. Experimental investigation on power output of different photovoltaic array configurations under uniform and partial shading scenarios. Energy 2017;127:438–53.

[9] Pendem Suneel Raju, Suresh Mikkili. Modelling and performance assessment of pv array topologies under partial shading conditions to mitigate the mismatching power losses. Sol Energy 2018;160:303–21.

[10] El-Dein MZ Shams, Kazerani Mehrdad, Salama MMA. Optimal photovoltaic array reconfiguration to reduce partial shading losses. IEEE Trans Sustain Energy 2013;4(1):145–53.

[11] La Manna Damiano, Li Vigni Vincenzo, Riva Sanseverino Eleonora, Di Dio Vincenzo, Romano Pietro. Reconfigurable electrical interconnection strategies for photovoltaic arrays: a review. Renew Sustain Energy Rev 2014;33:412–26.

[12] Sai Krishna G, Moger Tukaram. Reconfiguration strategies for reducing partial shading effects in photovoltaic arrays: State of the art. Sol Energy 2019;182:429–52.

[13] Singh Yadav Anurag, Kumar Pachauri Rupendra, Yogesh K Chauhan, Choudhury S, Singh Rajesh. Performance enhancement of partially shaded pv array using novel shade dispersion effect on magic-square puzzle configuration. Sol Energy 2017;144:780–97.

[14] Pachauri Rupendra, Singh Anurag, Yadav, Yogesh K Chauhan, Sharma Abhinav, Kumar Vinod. Shade dispersion-based photovoltaic array configurations for performance enhancement under partial shading conditions. Int Trans Elect Energy Syst 2018:1–32. e2556.

[15] Salameh Ziyad M, Dagher Fouad. The effect of electrical array reconfiguration on the performance of a pv-powered volumetric water pump. IEEE Trans Energy Convers 1990;5(4):653–8.

[16] Salameh Ziyad M, Liang Chaozi. Optimum switching points for array reconfiguration controller. 1990. p. 971–6.

[17] Nguyen Dzung, Lehman Brad. An adaptive solar photovoltaic array using model-based reconfiguration algorithm. IEEE Trans Ind Electron 2008;55(7):2644–54.

[18] Nguyen Dzung, Lehman Brad. A reconfigurable solar photovoltaic array under shadow conditions. 2008. p. 980–6.

[19] Şener Parlak Koray. Pv array reconfiguration method under partial shading conditions. Int J Electr Power Energy Syst 2014;63:713–21.

[20] Manjunath Matam Venugopal Reddy Barry, Avinash Reddy Govind. Optimized reconfigurable pv array based photovoltaic water-pumping system. Sol Energy 2018;170:1063–73.

[21] Rani B Indu, Saravana Ilango G, Nagamani Chilakapati. Enhanced power generation from pv array under partial shading conditions by shade dispersion using su do ku configuration. IEEE Trans Sustain Energy 2013;4(3):594–601.

[22] Rao Potnuru Srinivasa, Pattabiraman Dinesh, Ganesan Saravana Ilango, Chilakapati Nagamani. Positioning of pv panels for reduction in line losses and mismatch losses in pv array. Renew Energy 2015;78:264–75.

[23] Horoufiany Majid, Ghandehari Reza. Optimization of the sudoku based reconfiguration technique for pv arrays power enhancement under mutual shading conditions. Sol Energy 2017;159:1037–46.

[24] Malathy S, Ramaprabha R. A static pv array architecture to enhance power generation under partial shaded conditions. 2015. p. 341–6.

[25] Satpathy Priya Ranjan, Sharma Renu, Jena Sasmita. A shade dispersion interconnection scheme for partially shaded modules in a solar pv array network. Energy 2017;139:350–65.

[26] Satpathy Priya Ranjan, Jena Sasmita, Sharma Renu. Power enhancement from partially shaded modules of solar pv arrays through various interconnections among modules. Energy 2018;144:839–50.

[27] Belhaouas N, Ait Cheikh M-S, Agathoklis P, Oularbi M-R, Amrouche B, Sedraoui K, Djilali N. Pv array power output maximization under partial shading using new shifted pv array arrangements. Appl Energy 2017;187:326–37.

[28] Dhanalakshmi B, Rajasekar N. Dominance square based array reconfiguration scheme for power loss reduction in solar photovoltaic (pv) systems. Energy Convers Manag 2018;156:84–102.

[29] Pillai Dhanup S, Ram J Prasanth, Sai Nihanth Malisetty Siva, Rajasekar N. A simple, sensorless and fixed reconfiguration scheme for maximum power enhancement in pv systems. Energy Convers Manag 2018;172:402–17.

[30] John Bosco M, Mabel M Carolin. A novel cross diagonal view configuration of a pv system under partial shading condition. Sol Energy 2017;158:760–73.

[31] Dhanup S Pillai N Rajasekar, Ram J Prasanth, Kumar Chinnaiyan Venkatachalam. Design and testing of two phase array reconfiguration procedure for maximizing power in solar pv systems under partial shade conditions (psc). Energy Convers Manag 2018;178:92–110.

[32] Mittal Manan, Bora Birinchi, Saxena Sahaj, Anshu Mli Gaur. Performance prediction of pv module using electrical equivalent model and artificial neural network. Sol Energy 2018;176:104–17.

[33] Dkhichi Fayrouz, Oukarfi Benyounes, Fakkar Abderrahim, Belbounaguia Noureddine. Parameter identification of solar cell model using levenberg–marquardt algorithm combined with simulated annealing. Sol Energy 2014;110:781–8.

[34] Tian Hongmei, Mancilla-David Fernando, Ellis Kevin, Muljadi Eduard, Jenkins Peter. A cell-to-module-to-array detailed model for photovoltaic panels. Sol Energy 2012;86(9):2695–706.